DETERMINATION OF THALLIUM BY VOLATILE COMPOUND GENERATION ATOMIC ABSORPTION SPECTROMETRY

A THESIS SUBMITTED TO
THE GRADUATE SCHOOL OF NATURAL AND APPLIED SCIENCES
OF
MIDDLE EAST TECHNICAL UNIVERSITY

BY

SEVAL ATAMAN

IN PARTIAL FULFILLMENT OF THE REQUIREMENTS
FOR
THE DEGREE OF MASTER OF SCIENCE
IN
CHEMISTRY

SEPTEMBER 2011

Approval of the Thesis;

DETERMINATION OF THALLIUM BY VOLATILE COMPOUND GENERATION ATOMIC ABSORPTION SPECTROMETRY

Submitted by **SEVAL ATAMAN** in a partial fulfillment of the requirements for the degree of **Master of Science in Chemistry Department, Middle East Technical University** by

Prof. Dr. Canan Özgen
Dean, Graduate School of **Natural and Applied Sciences** _____

Prof. Dr. İlker Özkan
Head of Department, **Chemistry** _____

Prof Dr. O. Yavuz Ataman
Supervisor, **Chemistry Department, METU** _____

Examining Committee Members:

Prof. Dr. E. Hale Göktürk
Chemistry Department, METU _____

Prof. Dr. O. Yavuz Ataman
Chemistry Department, METU _____

Prof. Dr. Ali Gökmen
Chemistry Department, METU _____

Prof. Dr. Nusret Ertaş
Faculty of Pharmacy, Gazi University _____

Assoc. Prof. Dr. Uğur Tamer
Faculty of Pharmacy, Gazi University _____

Date: 09.09.2011

I hereby declare that all information in this document has been obtained and presented in accordance with academic rules and ethical conduct. I also declare that, as required by these rules and conduct, I have fully cited and referenced all material and results that are not original to this work.

Name, Last name: Seval Ataman

Signature

ABSTRACT

DETERMINATION OF THALLIUM BY VOLATILE COMPOUND GENERATION ATOMIC ABSORPTION SPECTROMETRY

Ataman, Seval

M.Sc., Department of Chemistry

Supervisor: Prof. Dr. O. Yavuz Ataman

September 2011, 69 pages

Determination of thallium is important due to its toxic effects on the environment and human health. Extremely low abundance of thallium in earth crust requires very sensitive and accurate methods for determination of this element. Although volatile compound generation is a sensitive, fast and economical method, thallium determination by this method has not been sufficiently investigated in literature, because of the fact that the formation of volatile forms of this element is a difficult task.

A continuous flow volatile compound generation system was developed and parameters that affect the analytical signal were optimized. Sample solutions were acidified with 0.5 mol/L HNO_3 and prepared in 0.0005% (v/v) rhodamine B and 1.0 mg/L Pd while 0.5% (m/v) $NaBH_4$ stabilized in 0.5% (m/v) NaOH was used as reductant. Fast decomposition and unstability of thallium volatile species affected system performance negatively.

Flow injection volatile compound generation studies were carried out with a special system. After optimizations, LOD and LOQ values were calculated as 12

ng/mL and 40 ng/mL according to peak height values in HNO_3 medium. Similarly, in HCl medium LOD and LOQ values were calculated as 14 ng/mL and 45 ng/mL. Addition of Te and Pd to the sample solution containing co-enhancement reagent rhodamine B improved volatile compound generation efficiency in peak height by 3.6 and 9.3, respectively. Type of the acid used was affected peak heights and peak shapes of Tl^+ and Tl^{3+} volatile species and HNO_3 medium gave better results.

By changing the location of introduction for Ar gas, the sources of memory effects and reasons of peak broadening were investigated. Most of the memory effects were coming from the gas-liquid separator (GLS) or before the GLS, as well as T-tube atomizer.

Nature and behavior of Tl volatile species were also investigated and it was found that Tl and also Pd were generated in the form of nanoparticles. Transmission electron microscopic (TEM) measurements prove the presence of Tl nanoparticles in the analyte species transported to the atomizer by the effect of carrier Ar gas.

Keywords: Thallium, volatile compound generation, enhancement reagent, memory effect, atomic absorption spectrometry

ÖZ

UÇUCU BİLEŞİK OLUŞTURMALI ATOMİK ABSORPSİYON SPEKTROMETRE İLE TALYUM ELEMENTİNİN TAYİNİ

Ataman, Seval

Yüksek Lisans, Kimya Bölümü

Tez Yöneticisi: Prof. Dr. O. Yavuz Ataman

Eylül 2011, 69 sayfa

Çevreye ve insan sağlığı üzerindeki toksik etkileri nedeniyle talyum elementinin tayini çok önemlidir. Doğada eser derişimlerde bulunan talyum elementinin tayini çok hassas ve doğru yöntemlerin kullanılmasını gerektirmektedir. Uçucu bileşik oluşturmalı atomik absorpsiyon spektrometri kolay, duyarlı ve ekonomik bir yöntem olmasına rağmen talyum tayininde fazla kullanılmamaktadır; bunun nedeni ise talyum için uçucu türleri oluşturmanın zor bir işlem olmasıdır.

Öncelikle sürekli akış uçucu bileşik oluşturmalı bir sistem geliştirilmiş ve analitik sinyali etkileyen parametreler optimize edilmiştir. Örnek çözeltiler 0.5 mol/L HNO_3, 0.0005% (v/v) rodamin B ve 1.0 mg/L Pd içerisinde hazırlanmıştır; 0.5% (m/v) NaOH içerisinde stabilize edilmiş $NaBH_4$ ise indirgeyici çözelti olarak kullanılmıştır. Kararsız ve hızlıca bozunan talyum uçucu türleri sistemin performansını olumsuz yönde etkilemiştir.

Akışa enjeksiyonlu uçucu bileşik oluşturma çalışmaları özel tasarlanmış bir sistemde yürütülmüştür. Gerekli parametrelerin optimizasyonlarından sonra HNO_3 ortamındaki gözlenebilme ve tayin sınırları sinyal yüksekliğine göre sırasıyla

12 ng/mL ve 40 ng/mL olarak hesaplanmıştır. Benzer şekilde HCl ortamındaki gözlenebilme ve tayin sınırları 14 ng/mL ve 45 ng/mL olarak hesaplanmıştır. Yardımcı reaktif olarak kullanılan rodamin B içeren örnek çözeltiye Te ve Pd elementlerinin eklenmesi uçucu bileşik oluşturma verimliliğini sırasıyla 3.6 ve 9.3 oranlarında arttırmıştır. Kullanılan asit türünün Tl^{+} ve Tl^{3+} uçucu türleri için sinyal şekli ve yüksekliğini etkilediği belirlenmiş ve HNO_3 içinde hazırlanmış çözeltilerden daha iyi sonuçlar elde edilmiştir.

Ar gazının sisteme giriş noktası değiştirilerek pik genişlemesi ve hafıza etkisinin sebepleri araştırılmıştır. Çalışmalar sonucunda T- tüp atomlaştırıcının da etkisi olmasına rağmen hafıza etkisinin büyük oranda gaz sıvı ayırıcı (GLS) ve öncesinden kaynaklandığı belirlenmiştir.

Tl uçucu türleri ve onların davranışlarının araştırıldığı çalışmada Tl ve Pd elementlerinin nano tanecikler halinde oluştuğu belirlenmiştir. Geçirmeli electron mikroskobu (TEM) ölçümleri Ar gazının yardımıyla atomlaştırıcıya taşınan türlerin Tl nano tanecikleri olduğunu kanıtlamıştır.

Anahtar Kelimeler: Talyum, uçucu bileşik oluşturma, yardımcı reaktif, hafıza etkisi, atomik absorpsiyon spektrometri

To My Family

ACKNOWLEDGEMENTS

I would like to express my gratitude to my supervisor Prof. Dr. O. Yavuz Ataman not only for his guidance, support, encouragement, patience and for teaching us how to become a good scientist but also for listening and helping us in many ways.

I would like to thank to Yasin Arslan for his ideas, constructive comments, guidance and contribution in each part of this study.

I am deeply grateful to Damla Parlar, Aida Nurioğlu, İlkem Evcimen and Erhan Özdemir for their endless help in my work, support and friendship.

I should also thank to Sezgin Bakırdere and all Ataman Research Group members for their understanding, patience, friendship and moral support.

Finally, my special appreciation and gratitude is devoted to my family for their trust, patience and moral support which makes everything possible.

TABLE OF CONTENTS

LIST OF TABLES

TABLES

LIST OF FIGURES

FIGURES

LIST OF ABBREVIATIONS

AAS	Atomic Absorption Spectrometry
AFS	Atomic Fluorescence Spectrometry
C_0	Characteristic Concentration
CHG	Chemical Hydride Generation
E	Enhancement Factor
ECHG	Electrochemical Hydride Generation
EHQTA	Externally Heated Quartz Tube Atomizer
ETAAS	Electrothermal Atomic Absorption Spectrometry
FAAS	Flame Atomic Absorption Spectrometry
GLS	Gas Liquid Separator
GTA	Graphite Tube Atomizer
HCL	Hollow Cathode Lamp
HG	Hydride Generation
HGAAS	Hydride Generation Atomic Absorption Spectrometry
HGAFS	Hydride Generation Atomic Fluorescence Spectrometry

HG-ETAAS	Hydride Generation Electrothermal Atomic Absorption Spectrometry
ICPMS	Inductively Coupled Plasma Mass Spectrometry
ICPOES	Inductively Coupled Plasma Optical Emission Spectrometry
INAA	Instrumental Neutron Activation Analysis
Id	Inner Diameter
LOD	Limit of Detection
LOQ	Limit of Quantification
PTFE	Polytetrafluoroethylene
QTA	Quartz Tube Atomizer
RSD	Relative Standard Deviation
VCGAAS	Volatile Compound Generation Atomic Absorption Spectrometry

CHAPTER 1

INTRODUCTION

1.1 Thallium

Thallium is an element with the symbol Tl, atomic number of 81, atomic mass of 204.4 g/mol, melting point of 304 ^{o}C and boiling point of 1473 ^{o}C. In 1861, thallium was discovered by Sir William Crookes from the residues of sulfuric acid plant. The name Thallium was originated from the Greek word *thallos* meaning "a green shoot or twig" due to its green spectral line. Thallium which is grayish white metal shows similar appearance to tin. This element is not only heavy but also soft and can be easily cut with a knife **(Blumenthal, Sellers, & Koval, 2006)**.

Nitric acid dissolves thallium and attacks this element considerably faster than dilute sulfuric acid. Because of low solubility of the salt, thallium is sparingly soluble in hydrochloric acid **(Blumenthal, Sellers, & Koval, 2006)**.

Tl^{+} and Tl^{3+} are the two oxidation states of thallium. Stability of Tl^{+} in aqueous solutions is higher; however, Tl^{3+} forms more stable complexes. Bioavailabity and toxicity properties of the two oxidation states are different **(Ensafı & Rezaei, 1998)**. It has been stated that the lower valency state is more toxic **(Ensafı & Rezaei, 1998)** and reactive than the trivalent state **(Florence, 1986)**. Determination of Tl^{+} in the environmental and biological samples is crucial since Tl^{+} ions exhibit more biological activation. It has been proven that in the activation of enzymes, Tl^{+} can be replaced

with potassium ions **(Hosseini, Chamsaz, Raissi, & Naseri, 2005)** since it is an analogue of potassium. The content of this element in the environment, its speciation and circulation is important since the toxicity, adsorption and transport properties can be affected by the redox state **(Pérez-Ruiz, Martínez-Lozano, Tomás, & Casajús, 1996)**. US Environmental Protection Agency introduces Thallium to the list of 13 priority metals due to its high toxic properties **(Scheckel, Lombi, Rock, & Mclaughlin, 2004; Keith, & Telliard, 1979)**

1.1.1 Occurrence and Production

The estimated abundance of thallium in the earth's crust is 0.1-1.7 mg/kg. Sulphide ores of zinc, copper and lead are the main sources. It is also present in granite, shale, limestone, sandstone and coal **(Kazantzis, 2000)**. Crookesite, lorandite and hutchinsonite are the most notable minerals containing low concentrations of thallium. In addition, very small quantities of this element exist in sea water and in certain mineral waters. For this reason, it is one of the rarer metals **(Anderson, 1953)**.

Thallium is discharged into the environment from the production of zinc, cadmium, and lead and by combustion of coal that increase pollution levels in nature **(Das, Chakraborty, Cervera, & Guardia, 2006)**. Cement production and fossil combustion stations are the principal sources that are responsible from pollution **(Hosseini, Chamsaz, Raissi, & Naseri, 2005)** and people living in the vicinity of these areas are subject to thallium poisoning.

1.1.2 Industrial Usage

Because of the fact that thallium is a toxic element its commercial applications are very limited. With many metals, it forms a number of binary, ternary, and quaternary eutectic alloys some of which have unique properties such as very low coefficients of friction and acid resistance. In bearings and contact points Ag-Tl and Au-Al-Tl, in the production of specific anodes Pb-Sn-Tl alloys have been used **(Blumenthal, Sellers, & Koval, 2006)**. Optical systems, low temperature thermometers, dye pigments, photoelectric cells and chemical synthesis **(Ensafı & Rezaei, 1998)**, electrical and electronics industries, as electronic devices for semi conductors, scintillation counters, mixed crystals for infrared instruments and laser equipment are the main fields that thallium is used **(Kazantzis, 2000)**.

1.1.3 Thallium and Health Effects

In spite of the fact that toxic effects of thallium were realized soon after its discovery, there is still very little information in the literature dealing with the prolonged exposures at low levels. It has been accepted that thallium is a cumulative poison and it has teratogenic and mutagenic properties **(Ebdon, Goodal, Hill, Stockwell, & Thompson, 1995)**. As being more toxic to mammals than the elements Hg, Cd and Pb, thallium has been stated as an important EPA priority pollutant **(Meeravali & Jiang, 2008)**.

Oral intake of 20-60 mg thallium/kg body weight within a week is fatal for an adult although this dose for humans is not proved yet **(Blumenthal, Sellers, & Koval, 2006)**. Inhalation of dust and fumes, ingestion of thallium contaminated food, and hand or skin contact cause chronic thallium poisoning with the symptoms of tiredness, fatique, headache and insomnia, nausea and vomiting, muscle and joint

pains, paraesthesia, numbness of fingers and toes **(Kazantzis, 2000)**. In short time exposures gastrointestinal irritation and disorders of the nervous system appears. In the long term blood chemistry changes and also liver, kidney, intestinal and testicular tissue are damaged **(Das, Chakraborty, Cervera, & Guardia, 2006)**. Hair loss and even death are also observed in prolonged and acute exposures **(Pavlíčkova, Zbíral, Smatanová, Habarta, Houserová, & Kubáň, 2006)**.

1.2 Atomic Absorption Spectrometry (AAS)

In the seventeenth century, history of optical spectroscopy began with the Sir Isaac Newton who observed the splitting of sunlight into various colors when it is passed through prism. Later, to understand the nature of light many studies have been performed and in 1802 black lines in the sun's spectrum were discovered by Wollaston. Fraunhofer investigated these blank lines and attributed letters to the strongest lines. Fraunhofer lines caused by absorption processes in the sun's atmosphere were later explained by Kirchhoff and Bunsen while studying on line reversal in the spectra of alkali and alkaline-earth elements (Figure 1).

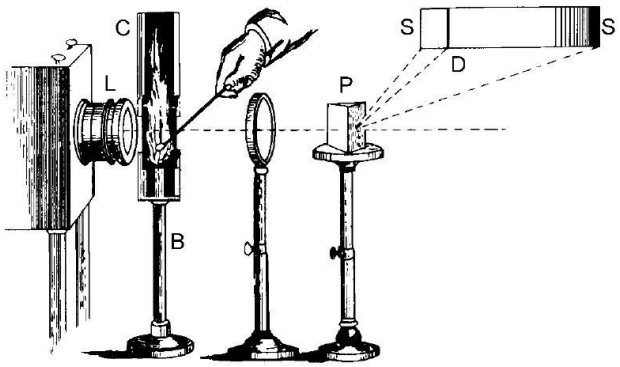

Figure 1 Experimental setup designed by Kirchhoff and Bunsen for the investigation of line reversal in the sodium spectrum (Welz & Sperling, 1999).

According to the law formulated by Kirchhoff, if any material emits radiation at a given wavelength, absorption of radiation for this material occurs in the same wavelength **(Welz & Sperling, 1999)**. Walsh and his colleagues developed hollow-cathode lamps for AAS and encouraged some small companies for the production of do-it-yourself atomic absorption spectrometers in the years between 1958 and 1962 **(L'vov, 2005)**.

In AAS, a radiation source which emits electromagnetic radiation specific to the analyte and an atom reservoir for introduction and atomization of the analyte are required. Ground-state atoms of the analyte absorb the resonant radiation coming from the radiation source and this absorption is used as the analytical signal **(Broekaert, 2005)**. Absorption of the electromagnetic radiation excites ground-state atoms to higher electronic state.

Among the atomic spectroscopy methods, AAS is the most popular one. It is not only well-established and robust method but also cheaper in terms of investment and running costs **(Dědina, 2010)**.

1.2.1 Flame Atomic Absorption Spectrometry (FAAS)

At the beginning years of AAS, for the atomization process flame atomizer was used and air/acetylene flame was preferred mostly rather than nitrous oxide/acetylene. Similarly, nebulization was a popular approach for the sample introduction **(Ataman, 2008)**.

The temperature of air/acetylene flame is not only high enough for sufficient atomization but also not so high to cause significant ionization interferences. In order to optimize the analytical conditions, composition of the burning gas mixture

can be changed. However, the temperature of air/acetylene flame is not enough for the atomization of more than 30 elements such as V, Ti, Zr, Ta and the lanthanides; nitrous oxide/acetylene flame is more suitable for these elements. Moreover, with different temperatures, air/propane, air/hydrogen and oxygen/acetylene flames are also available **(Broekaert, 2005)**.

For sample introduction, FAAS is mostly applied with pneumatic nebulizers. It is important that small droplets which are less than 10 µm in diameter must be generated in the nebulization system and then they are transported and completely vaporized in the flame. This enables high sensitivity and low magnitude of volatilization of the interferences **(Broekaert, 2005)**.

There are two important drawbacks affecting the sensitivity of FAAS. First one is relatively low efficiency of sample introduction system with the nebulization efficiency of 1-10%. Most of the sample is transported to the waste instead of atomizer and this causes dilution of the analyte concentration in the measurement zone in which the same volume is shared by source lamp beam and atoms. Secondly, analyte atoms have very short residence time in the measurement zone due to flame velocities and beam geometry **(Ataman, 2008)**.

1.2.2 Electrothermal Atomic Absorption Spectrometry (ETAAS)

The drawback coming from the low transport efficiency of the pneumatic nebulizers in FAAS has been overcome with ETAAS. In ETAAS, the sample is not transported to the flame; rather, it is placed into a small atomizer tube which is located on the optical path of the instrument **(Bakırdere, et al., 2011)**. The holders in ETAAS are usually graphite or metallic tube or cup furnaces. In this method, the sample is heated resistively in order to atomize the sample completely **(Broekaert, 2005)**. So

as to remove the solvent and contaminants before atomization, the temperature is increased step by step. Atomization of sample which has the volume of 10-50 µL takes place in a short time and a peak-shaped, time-dependent signal is obtained **(Welz & Sperling, 1999)**.

One disadvantage of ETAAS is the interferences in the atomization unit. In the determination of the analytes presenting in a heavy matrix such as environmental samples, interferences are the main problems that should be overcome. In addition, temperature profile of the graphite tube atomizers is not homogeneous while heating and the center of the tube is hotter than the edges. Inhomogeneous atomization of the analyte atoms results with the formation of the multiple peaks and peak broadening **(Bakırdere, et al., 2011; Frech, & Baxter, 1996)**.

1.3 Volatile Compound Generation Atomic Absorption Spectrometry (VCGAAS)

Liquid and gaseous phase sample introduction modes are commonly used in an atomic spectrometer. Gaseous-phase sample introduction techniques are generally based on formation of volatile compounds which are usually generated by a chemical reaction. In volatile compound generation technique, analyte in the liquid sample is converted to the gaseous phase by an appropriate reaction **(Dědina, 2010)**. Combination of AAS with volatile compound generation techniques offers several advantages compared to conventional nebulization methods such as improved selectivity, more efficient analyte atomization, elimination of nebulizer, and analyte preconcentration **(Arbab-Zavar, Chamsaz, Yousefi, & Ashraf, 2009)**. Volatilization of the species can be performed by cold vapor, hydridization, ethylation, propylation, halination, and photochemical vapor generation **(Bakırdere, et al., 2011)**. Elements determined by various chemical volatile compound

generation techniques are shown in Table 1 **(Tsalev, 1999)**. Among these techniques hydride generation has the greatest popularity.

Table 1 Chemical Vapor Generation in AAS (Tsalev, 1999).

Chemical system for vapour generation	Analyte[a]
Hydride generation (HG)	***As***, ***Bi***, ***Ge***, (In), Pb, ***Sb***, ***Se***, ***Sn***, ***Te***, (Tl)
Cold vapour (CV) technique	Cd, ***Hg***, (Cu?)
Ethylation	Bi, Cd, Co, Ge, ***Hg***, ***Pb***, ***Se***, ***Sn***, Tl
Butylation	Be, Ga, ***Hg***, ***Pb***, ***Sn***, Zn
Carbonyl generation	Co, Fe, ***Ni***
Chlorides	As, Bi, Cd, Ge, Mo, Pb, Sn, Tl, Zn
Fluorides	Ge, Mo, Re, U, V, W
Dithiocarbamates	Co, Cr, Cu
β-Diketonates	Al, Co, Cr, Cu, Fe, Mn, Ni, Pb, Zn
Miscellaneous VG techniques	***$B(CH_3O)_3$***, OsO_4

[a]Species in bold itallic indicate straightforward analytical performance; species in parantheses indicate serious problems with that particular analyte.

1.3.1 Hydride Generation Atomic Absorption Spectrometry (HGAAS)

Hydride generation is defined as hydride release from the sample solution. In this process, the analyte in an acidified sample solution is converted to hydride and transferred to the gaseous phase. After that, released hydride is transported to the

atomizer by the help of carrier gas **(Dědina & Tsalev, 1995)**. Hydride generation technique consists of four steps:

a) Generation of the hydride

b) Collection of the hydride

c) Transfer of the hydride

d) Atomization of the hydride

Efficiency of each step affects the sensitivity of the system **(Kumar & Riyazuddin, 2010)**. As, Pb Bi, Ge, Sn Sb, Se, and Te form analytically important hydrides and some physical properties and hydrides of these elements are shown in Table 2 **(Dědina & Tsalev, 1995)**.

Table 2 Molecular formulas and physical properties of some hydrides (Dědina & Tsalev, 1995).

Element	Name	Formula	Melting Point, ^{o}C	Boiling Point, ^{o}C	Solubility in Water (μg/mL)
As	Arsine	AsH_3	-116.3	-62.4	696
Bi	Bismuthine	BiH_3	-67	16.8	-
Ge	Germane	GeH_4	-164.8	-88.4	Insoluble
Pb	Plumbane	PbH_4	-135	-13	-
Sb	Stibine	SbH_3	-88	-18.4	4100
Se	Hydrogen Selenide	H_2Se	-65.7	-41.3	37700-68000
Sn	Stannane	SnH_4	-146	-52.5	-
Te	Tellurium Hydride	H_2Te	-51	-4	Very Soluble

Hydride generation is usually based on reduction reaction of the metalloid or metal. Sodium tetrahydroborate in acidic medium or zinc metal are commonly used as chemical reducing agent for the production of nascent hydrogen.

$Zn + 2H^+ \rightarrow Zn^{2+} + 2H$

$BH_4^- + H^+ + 3H_2O \rightarrow H_3BO_3 + 8H$

$A^{m+} + (m+n)\,H \rightarrow AH_n + mH^+$

Nascent hydrogen plays role in metal or metalloid reduction and hydride formation **(Dědina, 2010)**. On the other hand, opponents of this idea claimed that nascent hydrogen plays no role in the reduction process. In the generation process hydrogen with no special reducing capacity is involved and generation of hydrides can be considered as hydrogenation process **(Laborda, Bolea, Baranguan, & Castillo, 2002)**.

Tetrahydroborate/acid reaction is usually preferred to metal/acid reaction due to its inherent advantages based on reaction time, reduction yield, and blank contamination **(Dědina, 2010)**.

Hydride generation is one of the most frequently used techniques for the determination of trace elements mentioned above. The technique enables speciation analysis of the hydride forming elements. In addition, separation of the analyte from the matrix reduces interferences and also improves detection power **(Kumar & Riyazuddin, 2010)**. High transport efficiency and selectivity are also important advantages. Using this technique, gas phase separation methods such as gas chromatography can be employed in the speciation analysis of some elements **(Sturgeon, Guo, & Mester, 2005)**.

The steps of chemical reaction and hydride formation, separation of the volatile compounds from the liquid solution, and atomization process are the sources of interferences in hydride generation technique. There are four important factors affecting significance of interferences.

- The design of hydride generation system
- Acid and reducing agent concentrations
- The mixing order of reagents
- Atomizer type

The main sources of these interferences are shown on Figure 2 and categorized as gas phase and liquid phase **(Kumar & Riyazuddin, 2010)**.

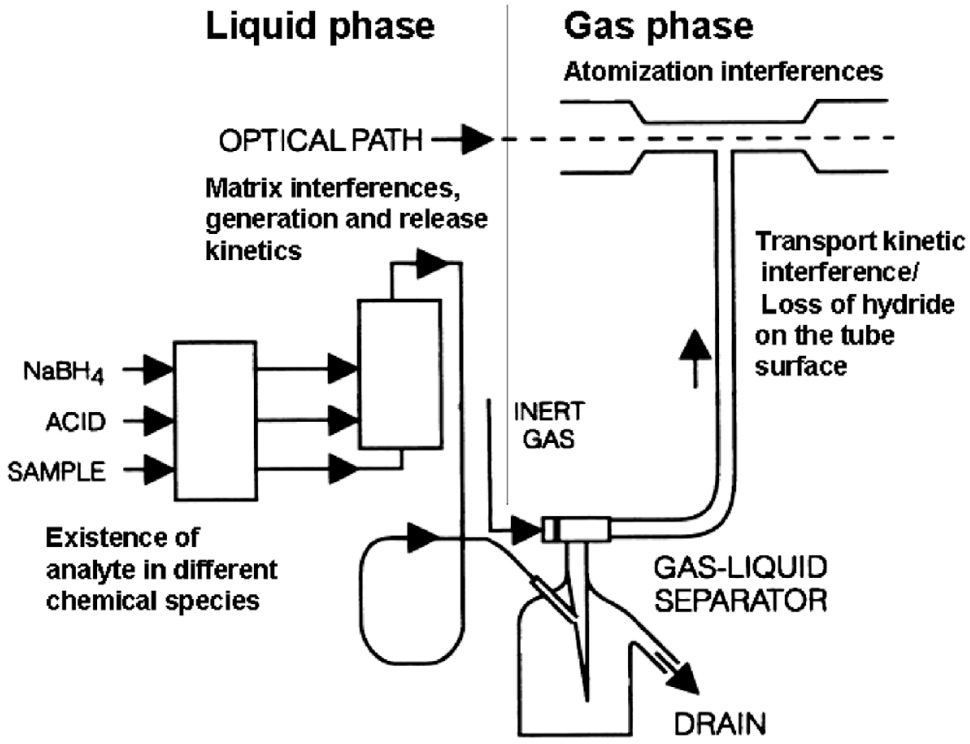

Figure 2 Stages of hydride generation causing several interferences (Kumar & Riyazuddin, 2010).

There are some difficulties in the detection of noble and transition metals. The nature and behavior of these elements is not clear. Because of unstability problem

and fast reaction conditions, mixing of the reagents and their separation must be as fast as possible **(Pohl, 2004)**.

1.4 Systems for Hydride Generation

There are several systems designed to determine hydride forming elements by volatile compound generation AAS. Batch and flow systems has been frequently used systems for this purpose.

1.4.1 Batch Systems

A glass or plastic vessel is used as the hydride generator and gas-liquid separator (GLS) in batch systems. An example of batch generator can be seen in Figure 3. Sample solution prepared in the acidic medium is placed inside the vessel and by the injection of reductant solution hydrides begin to form. The carrier gas is introduced to the system to separate volatile species from the liquid phase and to transport these species to the atomizer used **(Dědina & Tsalev, 1995)**.

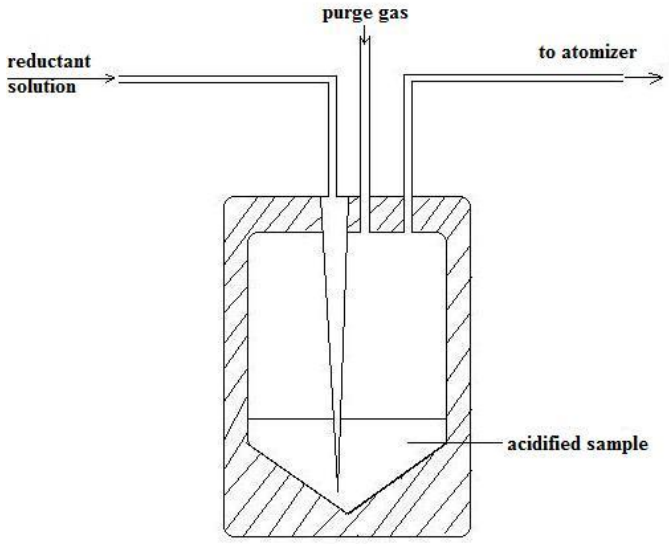

Figure 3 Schematic representation of hydride generation using batch system (Dědina & Tsalev, 1995).

The signal obtained in batch systems is proportional to the mass of the analyte in the sample solution. With the addition of reductant solution, pH value and also volume of hydrogen generation change with time. Changes in the hydride forming efficiency during measurement affect the signal shape and integration will be difficult. For this reason, using peak height measurements are generally preferred **(Welz & Sperling, 1999)**.

1.4.2 Flow Systems

Because of the fact that batch hydride generation systems operate manually, they require more time and effort. The drawbacks of batch systems are eliminated in continuous flow and flow injection systems which are automated systems. On the contrary to the batch systems, reactions take place in the tubes and volatile species are separated in the gas-liquid separators **(Welz & Sperling, 1999)**.

1.4.2.1 Continuous Flow Systems

A constant flow of acidified sample solution, constant flow of reductant solution, and carrier gas are mixed within the tube which is long enough to complete the reaction. After that, the mixture is sent to the gas-liquid separator. Volatile hydride species and carrier gas are separated from the liquid phase and transported to the atomizer **(Dědina & Tsalev, 1995)**.

In continuous flow systems, absorbance depends on concentration and signals obtained are time-independent. Increasing the sample flow rate increases the sensitivity; however, higher flow rates decrease separation and transport efficiencies of volatile species **(Welz & Sperling, 1999)**. Sample and reductant flow rates, sample acidity, gas flow rate, analyte concentration and transport efficiency are the factors affecting hydride supply function. Length of reaction coil is also important. It should be long enough to complete the reaction properly **(Dědina & Tsalev, 1995)**.

The most important advantage of continuous flow systems is that reagents are mixed with better pH control compared to batch systems. In addition when the system reaches equilibrium, constant output signal is obtained **(Campbell, 1992)**.

1.4.2.2 Flow Injection Systems

Working principle of flow injection systems is very similar to continuous flow systems. The difference is that carrier solution and reductant are sent at constant flow rates and a small volume of acidified sample solution is injected to the mixture at regular intervals. Experimental set-up remains the same as in continuous flow systems **(Welz & Sperling, 1999)**.

In flow injection systems, a peak-shaped signal with some degree of tailing is obtained **(Broekaert, 2005)**. Increasing injected sample volume and decreasing flow rate of carrier gas, in some case, help to improve the sensitivity **(Dědina & Tsalev, 1995)**.

1.5 Determination of Thallium

Since thallium is present in samples at very low concentrations, accurate and sensitive methods are required for the determination of low concentrations in environmental and biological samples. Inductively coupled plasma mass spectrometry (ICP-MS), laser-excited atomic florescence spectrometry (LEAFS), electrothermal atomic absorption spectrometry (ETAAS), flame atomic absorption spectrometry (FAAS), hydride generation atomic absorption spectrometry (HGAAS), hydride generation integrated atom trap flame atomic absorption spectrometry (HG-IAT-FAAS), flow injection hydride generation atomic absorption spectrometry (FI-HGAAS), electrochemical hydride generation (ECHG), potentiometry and voltammetry are usually applied for the determination of thallium.

Although ICP-MS offers sensitive results, it is an expensive analytical method due to high running costs. There are only few studies in literature using LEAFS for determination of thallium **(Dadfarnia, Assadollahi, & Haji Shabani, 2007)**. ETAAS offers several advantages such as low detection limit (LOD) and usability of low sample volumes; however, it suffers from several interferences that make appearance of errors inevitable **(Hosseini, Chamsaz, Raissi, & Naseri, 2005)**. For instance, in order to eliminate the interferences coming from the presence of sodium chloride and iron, addition of different matrix modifiers is offered **(Salvin, & Manning, 1980; Shan, Ni, & Zhang, 1984; Vale, Silva, Welz, & Newka, 2002; Zendelovska, & Stafilov, 2001)**. Stripping voltammetry is also one of the methods

that suffers from interferences by other metals, especially cadmium in thallium determination despite its high sensitivity and ability to detect the redox species of metals **(Arbab-Zavar, Chamsaz, Yousefi, & Ashraf, 2009; Zen, & Wu, 1997)**. FAAS is a simple and low cost method; however, in the determination of thallium low sensitivity of this method for its trace determination at μg/L level is the main problem. In most cases this can be handled by preconcentration **(Dadfarnia, Assadollahi, & Haji Shabani, 2007)**. Liquid-liquid extraction **(Asami, Mizui, Shimada, & Kubota, 1996)**, hydride generation **(Zhu & Xu, 2000)**, solid phase extraction **(Lin & Nriagu, 1999)** and flotation **(Hosseini, Chamsaz, Raissi, & Naseri, 2005)** are the most frequently used methods for the preconcentration and separation stages.

Yan et al. **(Yan, Yan, Cheng, & Li, 1984)** developed a batch hydride generation AAS method for the determination of thallium with the characteristic mass of 2.9 μg. They also pointed out that Te had the greatest effect on sensitivity among other hyride-forming elements such as As, In and Pb. Addition of Te improved characteristic mass to 0.12 μg. Liao et al. In another study, **(Liao, Chen, Yan, Li, & Ni, 1998)** researchers combined hydride generation and *in situ trapping in graphite tube systems for the ETAAS* determination and obtained a characteristic mass of 0.92 ng. They used Te as the enhancement reagent. Ebdon et al. **(Ebdon, Goodal, Hill, Stockwell, & Thompson, 1995)** developed a continuous flow method for HGAAS with the characteristic concentration of 4 ng/mL. However, noisy signals, several memory effects and variable peak shapes were the main problems. The excess noise was eliminated by cooling the reactants to the ice point prior to reaction.

1.6 Aim of the Study

Although interest in Tl determination has increased considerably in recent years, most of the proposed methods used for this purpose lack the sensitivity required for environmental samples. The main purpose of this study is to develop a sensitive analytical technique for thallium determination and investigate the nature of thallium volatile species. This will be achieved by using the advantages of flow injection VCG method. By optimizing the parameters, quality of the analytical signal obtained from Tl volatile species will be improved. After that, behavior and nature of this volatile species will be examined by employing transmission electron microscope (TEM) and energy dispersive X-ray spectrometry (EDS).

CHAPTER 2

EXPERIMENTAL

2.1 Chemicals and Reagents

All reagents used during the studies were of analytical grade or higher purity. Tl standard solutions used throughout the experiments were prepared daily by making appropriate dilutions from the 1000 mg/L stock solutions of Tl^{+} and Tl^{3+} (High Purity, Charleston). A 1000 mg/L Pd stock solution was prepared by dissolving solid $K_2(PdCl_6)$ in 1.0 mol/L HNO_3. Working solutions of Te were prepared by making dilutions from the 1000 mg/L stock solution of Te (Merck, Germany). Stock solution of %0.1 (m/v) rhodamine B (Allied Chemical, Morristown) was prepared weekly in deionized water and stored in refrigerator at dark. In order to acidify analyte solutions, analytical grade 65% (w/w) HNO_3 (Merck) and %37 (w/w) HCl (Merck, Germany) were used. Appropriate amount of powdered proanalysis grade $NaBH_4$ (Merck, Darmstadt, Germany) was dissolved in 0.5% NaOH (Riedel, Germany) for the preparation of reductant solution. Solution was used directly without filtration. Dilutions were made using 18 MΩ·cm deionized water obtained from a Millipore (Molsheim, France) Milli-Q water purification system which was fed using the water produced by Millipore Elix 5 electro deionization system. High purity Ar (99.999 %) was used as carrier gas throughout the study.

All the glass and plastic apparatus were kept in 10% (v/v) HNO_3 and rinsed with deionized water before use so as to remove the all kind of contaminations; nitric

acid solution was prepared by 1+9 dilution of the concentrated reagent with distilled water.

2.2 Atomic Absorption Spectrometer

For continuous flow and flow injection hydride generation studies a Varian AA140 (Victoria, Australia) atomic absorption spectrometer was used. The instrument was equipped with a deuterium arc background correction system and 10.0 cm burner head. Controlling and data processing was done with SpectrAA software (version 5.1). A Perkin Elmer uncoded Tl hollow cathode lamp was used as the radiation source. The parameters of the instrument that are used in the experiments are shown in Table 3.

Table 3 Operating conditions of AA spectrometer

Parameter	**Value**
Measurement Wavelength, nm	276.8
Spectral Bandpass, nm	0.5
Lamp Current, mA	5.0
Flame Type	Stoichiometric Air/Acetylene
Measurement Mode	Integration

2.3 Continuous Flow Volatile Compound Generation System

$NaBH_4$ solution which is used as reductant and acidified sample solution are pumped using yellow-blue color coded 1.27 mm id Tygon® peristaltic pump tubings. Solutions are sent at constant flow rates by the help of Gilson Minipuls 3 (Villers Le Bell, France) 4-channel peristaltic pumps. Waste solution is removed from the system by Gilson Minipuls 3, 4-channel peristaltic pump. Carrier gas is introduced to the system by the help of mass flow controller (Cole Palmer, USA). Continuous flow VCG system used during the studies is shown in Figure 4.

For the junction points of tubings and carrier gas, 3 way T-shaped PTFE connectors (Cole Palmer, Illinois, USA) were used. PTFE connection tubings (Cole Palmer) with 0.56 mm i.d. were used for the reaction and stripping coils.

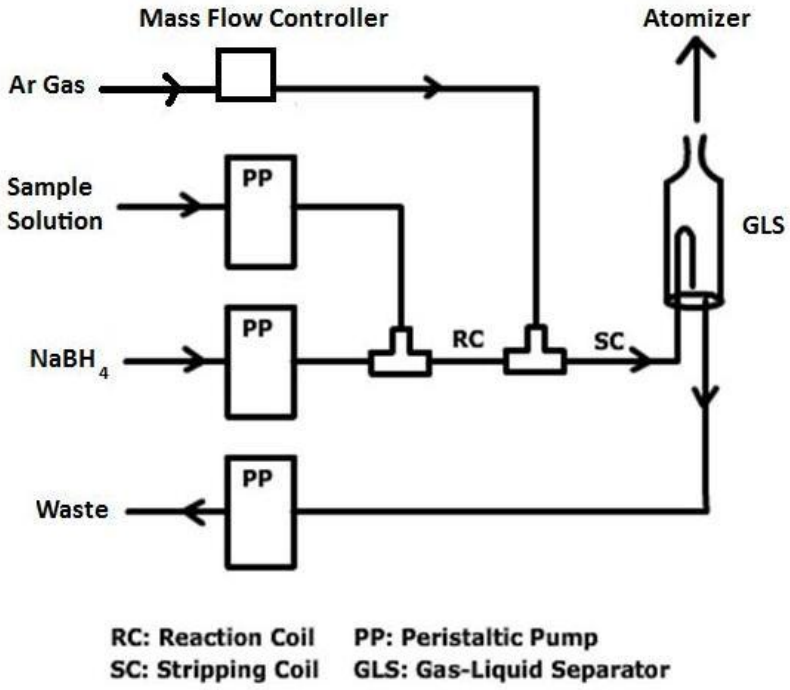

Figure 4 Schematic representation of the continuous flow volatile compound generation system.

So as to separate liquid and gaseous phases, laboratory made borosilicate gas-liquid separator was placed after stripping coil. Schematic representation and dimensions of the GLS are shown in Figure 5. Formed volatile species were transported to the atomization unit by the help of 15.0 cm length 6.0 mm i.d. PTFE tubing.

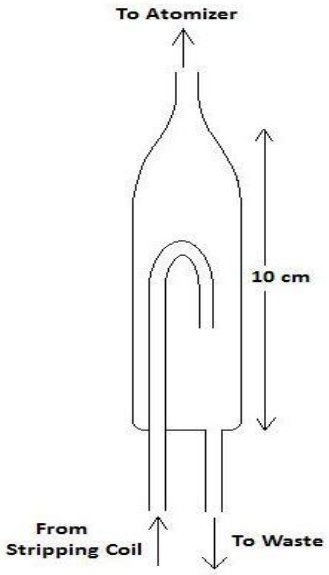

Figure 5 Schematic representation of GLS used in continuous flow system.

An externally heated T-shaped quartz tube atomizer (Çalışkan Cam, Ankara, Turkey) was used as the atomization unit throughout the study; its dimensions are given in Figure 6. Quartz tube atomizer (QTA) consisted of a horizontal arm and an inlet arm. Horizontal arm of the QTA was aligned in the optical path of the instrument and placed 3.0 mm above the burner head by using QTA holding apparatus. Volatile species are transported to the atomizer by the help of inlet arm.

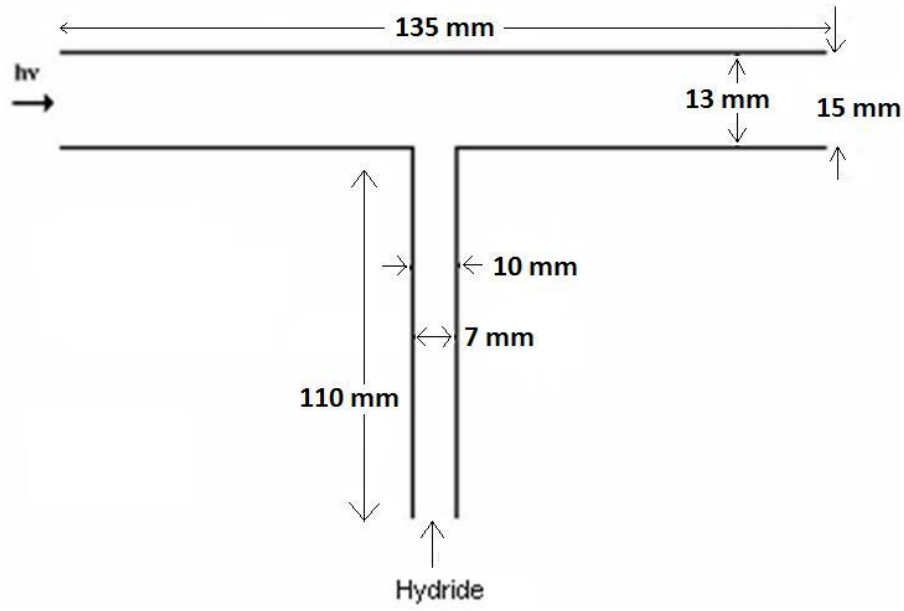

Figure 6 Schematic representation of externally heated quartz tube atomizer.

New T-tubes were conditioned by using 100 mL of 10.0 mg/L Tl solution with the continuous flow VCG method. Sample solution was prepared in 0.5 mol/L HNO_3, 0.005% (m/v) rhodamine B and 1.0 mg/L Pd. 3.0% (m/v) $NaBH_4$ stabilized in 0.5% (m/v) NaOH was used as reductant and merged with the sample solution through reaction coil. Ar was sent with the flow rate of 50.0 mL/min. The reason of conditioning new tubes before using is to saturate T-tube and prevent fluctuations in the signals.

2.4 Flow Injection Volatile Compound Generation System

Carrier solution and $NaBH_4$ solution are pumped through yellow-blue color coded 1.27 mm id Tygon® peristaltic pump tubings by the help of Gilson Minipuls 3, 4-

channel peristaltic pumps. A manual injection valve with a 400 µL sample loop was used to inject the sample to the flow injection system.

During the studies, a special design flow injection system was used **(Musil et al., 2010; Arslan et al., 2010)**. 1/16" o.d. PTFE tubings and ¼-28 PEEK connectors are employed for the construction of the system. 3 concentric capillaries and a special GLS formed the basis of the flow injection system (Figure 7). 0.25 mm i.d. quartz innermost capillary carried injected sample and carrier solution. 0.53 mm i.d. quartz middle capillary was used for $NaBH_4$ solution. Carrier gas was sent through 1 mm i.d. PTFE outer capillary. The edges of these concentric capillaries ended at 1 mm distance from each other and protrude 5 mm inside the glass GLS. The volume of the GLS was 3 mL which was a very small volume for a GLS compared to the conventional ones. Mixing of reagents coming from the capillaries took place into this small volume and by the help of carrier gas volatile species were transported to the T-tube where the atomization occurred. 4.0 cm length 3.0 mm i.d. PTFE tubing was used to connect the exit point of GLS and inlet arm of T-tube.

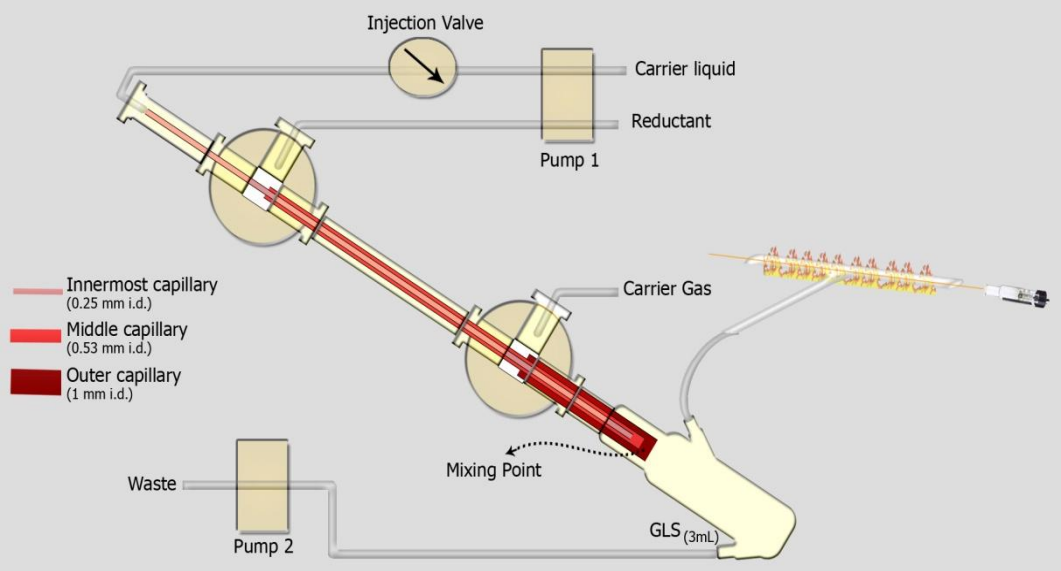

Figure 7 Schematic representation of the flow injection volatile compound generation system.

The main characteristic of the system was the fast separation of the Tl volatile species from the solution. On the contrary to other VCG systems, there were no reaction and stripping coils. Reagents were mixed in a small volume and volatile species were transported to the atomizer very quickly. By this way, most of the memory effect coming from the reaction and stripping coils were eliminated. Moreover, using small volume of GLS also reduced the memory effect coming from the adsorptions on the glass surface.

2.5 Procedures

2.5.1 Continuous Flow Volatile Compound Generation

For the continuous flow VCG system, sample and $NaBH_4$ flow rates were optimized and used as 1.6 mL/min and 2.5 mL/min, respectively. Sample solution was acidified with HNO_3 to get a final solution 0.5 mol/L HNO_3. Pd and rhodamine B were added to the acidified sample solution to a final concentration of 1.0 mg/L and 0.0005% (m/v), respectively. Reductant solution was made up of 6.0% (m/v) $NaBH_4$ in 0.5% (m/v) NaOH solution and it was merged with sample solution through 35.0 cm length reaction coil. Carrier gas was sent with the optimized flow rate of 50 mL/min and added to the system through 25.0 cm length stripping coil. An integrated signal was collected for 10 seconds and each result was the mean of at least two replicate measurements.

2.5.2 Flow Injection Volatile Compound Generation

So as to reach low detection limits in flow injection VCG system, parameters affecting VCG efficiency were optimized by using 1.0 mg/L Tl solution. 0.5 mol/L HNO_3 was used as the carrier solution. Reductant solution was made up of 3.0% (m/v) $NaBH_4$ in 0.5% (m/v) NaOH and carrier gas flow rate was set to 50 mL/min. Carrier solution and $NaBH_4$ were sent with the flow rates of 1.0 mL/min. $NaBH_4$, carrier gas and the carrier solution containing sample plug were mixed at the entrance point of the GLS. Generated volatile species were transported to the atomizer by the help of carrier gas. Blank solution containing 0.5 mol/L HNO_3, 0.005% (m/v) rhodamine B and 1.0 mg/L Pd was used to control the memory effect.

CHAPTER 3

RESULTS AND DISCUSSION

This study involves development of sensitive analytical methods for the determination of thallium at low detection limits.

First part of the study includes quantitative determination of thallium by continuous flow volatile compound generation AAS system. In this part $NaBH_4$, sample and Ar flow rates, $NaBH_4$ and HNO_3 concentrations were optimized. Because of black precipitates formed on the reaction and stripping coils, sensitivity and reproducibility of the method were affected and further development could not be done.

Second part consists of determination of thallium by a special flow injection volatile compound generation AAS system. In this system, black precipitates causing memory effect were eliminated and reproducible signals were obtained. Volatile compound generation efficiency of thallium was improved by optimizing the parameters. In addition, effects of enhancement reagents on volatile compound generation efficiency were also investigated.

Third part involves investigation of reasons of peak broadening in the signals. By changing the direction of Ar gas, the sources of memory effects causing peak broadening in the signals were examined.

The last part involves qualitative characterization of volatile thallium species. Samples adsorbed on the carbon/formvar coated Cu grids were examined in transmission electron microscope and presence of Tl nanoparticles was proven.

3.1 Continuous Flow Volatile Compound Generation System

In this part of the study, volatile species were generated in continuous mode and parameters were optimized to increase sensitivity.

3.1.1 Optimization of $NaBH_4$ and Sample Solution Flow Rates

10.0 mg/L Tl was chosen as the starting concentration and sample solution was prepared in 0.5 mol/L HNO_3, 0.0005% (m/v) rhodamine B and 1.0 mg/L Pd. $NaBH_4$ solution was made up of 1.0% (m/v) $NaBH_4$ in 0.5% (m/v) NaOH. Ar flow rate was set to 200 mL/min and kept constant during the experiment. 1.1 mL/min sample flow rate was kept constant and $NaBH_4$ flow rate was varied between 1.1 mL/min and 3.3 mL/min to determine optimum flow rate. Results given in Figure 8 illustrate that $NaBH_4$ flow rate had a significant effect on VCG efficiency since absorbance value increased about 9 times when $NaBH_4$ flow rate was increased from 1.1 mL/min to 2.5 mL/min which was found as optimum.

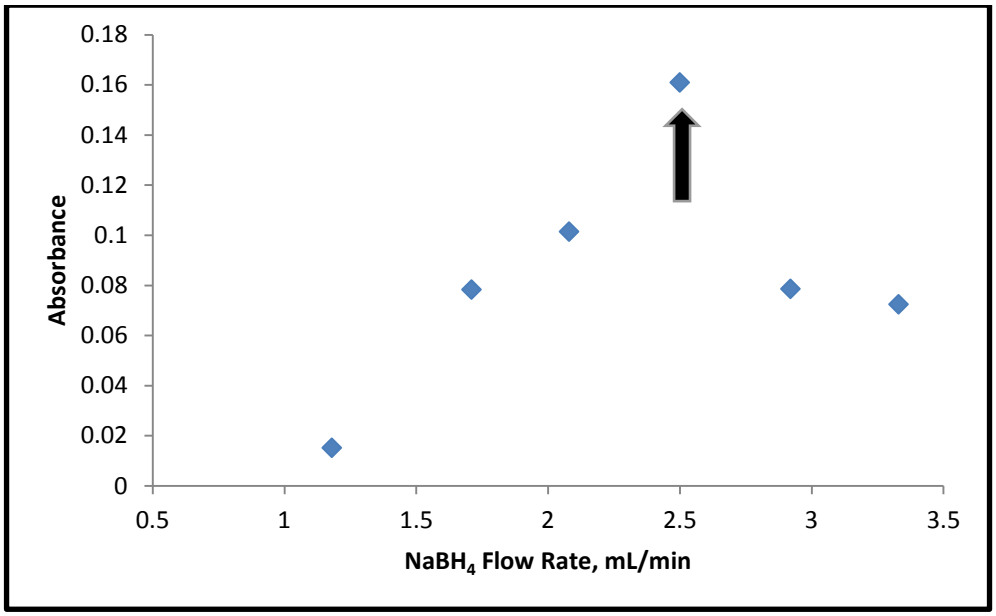

Figure 8 Effect of $NaBH_4$ flow rate on the continuous flow VCGAAS signal of 10.0 mg/L Tl solution prepared in 0.5 mol/L HNO_3, 0.0005% (m/v) rhodamine B and 1.0 mg/L Pd. Sample and Ar were sent with the flow rates of 1.1 mL/min and 200 mL/min, respectively. 1.0% (m/v) $NaBH_4$ in 0.5% (m/v) NaOH was used.

After that, 2.5 mL/min $NaBH_4$ flow rate was kept constant and effect of sample flow rate was investigated by varying the flow rate between 1.1 mL/min and 3.2 mL/min. Results shown in Figures 8 and 9 indicate that optimum flow rates for $NaBH_4$ and sample solution were 2.5 mL/min and 1.6 mL/min, respectively.

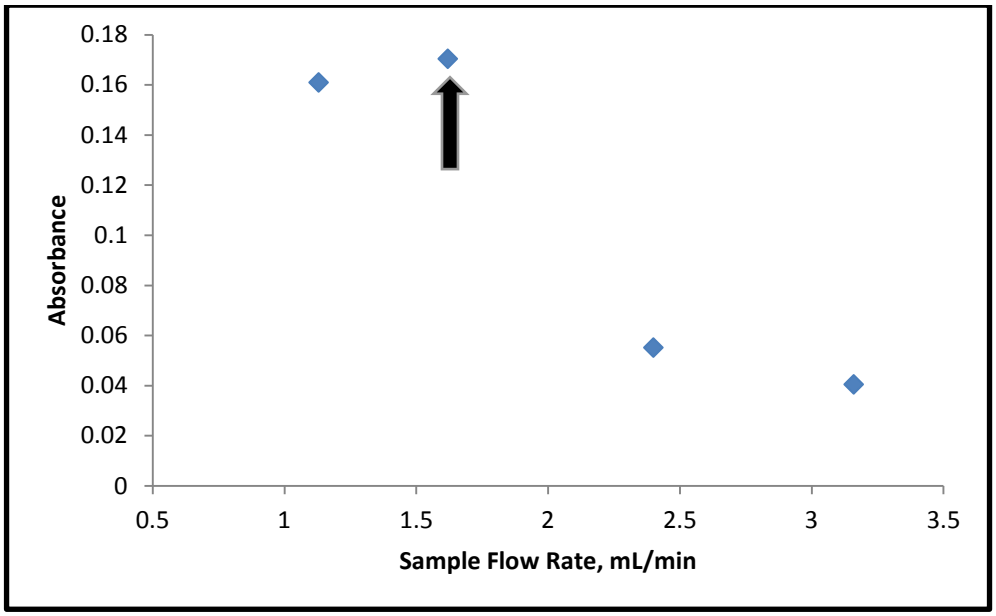

Figure 9 Effect of sample flow rate on the continuous flow VCGAAS signal of 10.0 mg/L Tl solution prepared in 0.5 mol/L HNO_3, 0.0005% (m/v) rhodamine B and 1.0 mg/L Pd. 1.0% (m/v) $NaBH_4$ in 0.5% (m/v) NaOH was used with a flow rate of 2.5 mL/min. Ar flow rate was set as 200 mL/min.

3.1.2 Optimization of Ar Flow Rate

The function of carrier gas is to transport volatile species to the atomizer. Moreover, it may also help to strip volatile species out of sample solution. Carrier gas is chosen with respect to atomizer performance and optimum economy **(Dědina & Tsalev, 1995)**. Carrier gas flow rate is one of the critical factors for system performance since flow stability and flow rate affect the sensitivity and repeatability of the method. Unstable gas flow rates cause fluctuations in the signals. For the determination of Tl by VCG method, Ar was selected as the carrier gas. Effect of Ar flow rate on absorbance values was examined with different flow rates varying from 25.0 mL/min to 300 mL/min. Absorbance value obtained in the absence of Ar gas

was also studied and 50.0 mL/min flow rate gave the best absorbance (Figure 10). Experimental results showed that higher Ar flow rates results in low absorbance values. The reason of signal decrease at higher flow rates is due to dilution effect of the gas. Moreover, it may also affect residence time of the atoms in the measurement zone. Signal decrease in the absence of Ar gas verified that it plays an important role in the transportation of volatile Tl species to the atomizer.

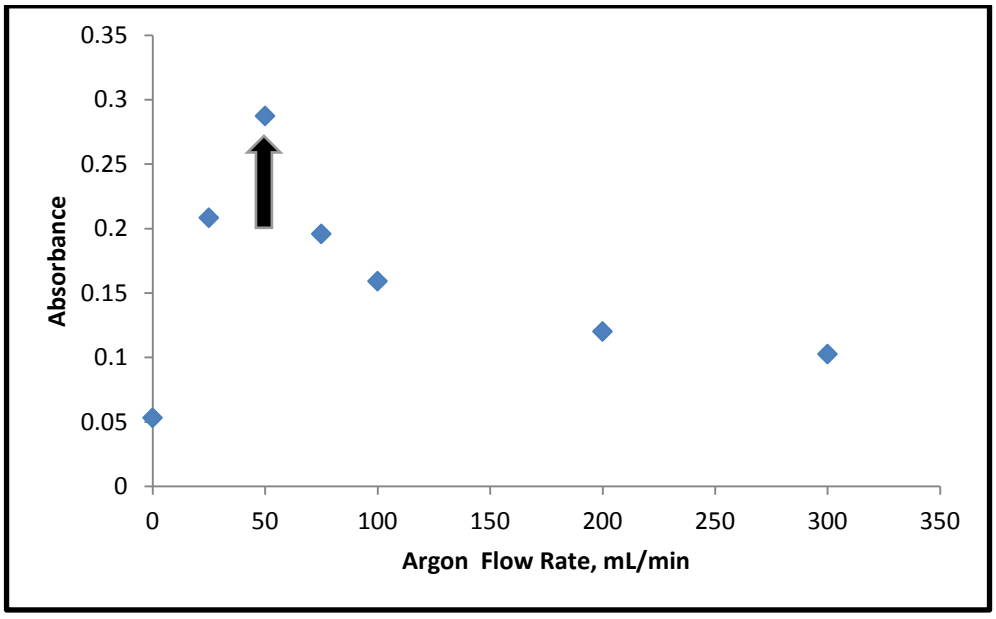

Figure 10 Effect of Ar flow rate on the continuous flow VCGAAS signal of 10.0 mg/L Tl solution prepared in 0.5 mol/L HNO_3, 0.0005% (m/v) rhodamine B and 1.0 mg/L Pd. Sample flow rate was 1.6 mL/min. 1.0% (m/v) $NaBH_4$ in 0.5% (m/v) NaOH was used with a flow rate of 2.5 mL/min.

3.1.3 Optimization of $NaBH_4$ Concentration

Reductant solution and acid concentrations become important in optimizations due to their significant effects on volatile compound generation efficiency of Tl. To see

the effect of $NaBH_4$ concentration, HNO_3 concentration of sample solution was kept constant as 0.5 mol/L and $NaBH_4$ solutions ranging from 1.0% (m/v) to 8.0% (m/v) were prepared. All $NaBH_4$ solutions were stabilized in 0.5% (m/v) NaOH. Results shown in Figure 11 indicated that increasing $NaBH_4$ concentration has a positive effect on analytical signal and gives rise to rapid and efficient formation of volatile species. VCG efficiency of Tl reached maximum with 6.0% (m/v) $NaBH_4$ merged with 0.5 mol/L HNO_3. This behavior may be explained by the fact that higher $NaBH_4$ concentrations results in increased hydrogen radicals in the measurement zone.

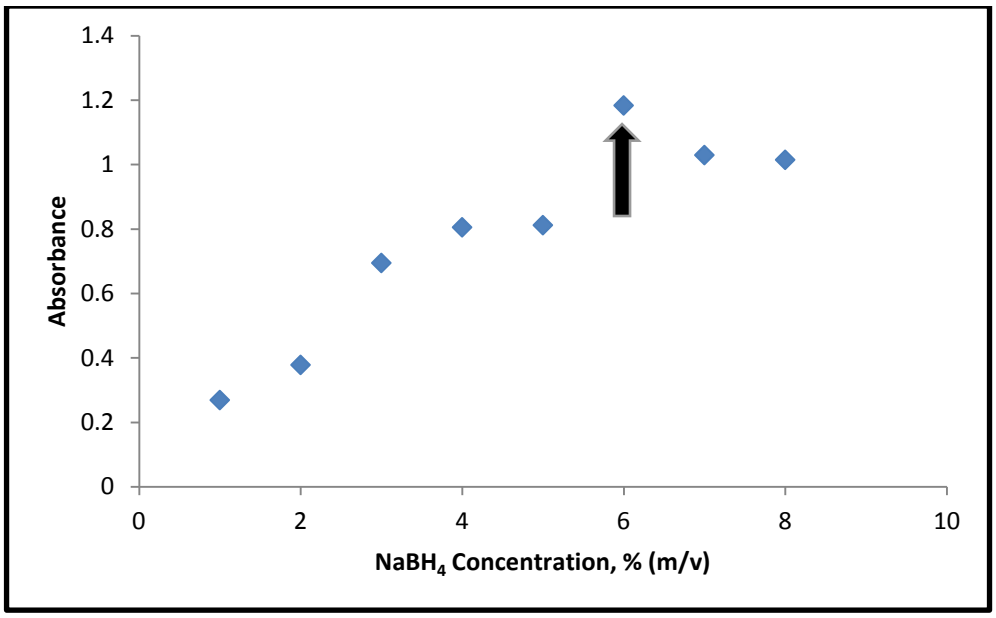

Figure 11 Effect of $NaBH_4$ concentration on the continuous flow VCGAAS signal of 10.0 mg/L Tl solution prepared in 0.5 mol/L HNO_3, 0.0005% (m/v) rhodamine B and 1.0 mg/L Pd. 50.0 mL/min Ar flow rate was used. Sample and $NaBH_4$ flow rates were set as 1.6 mL/min and 2.5 mL/min, respectively. $NaBH_4$ solutions were stabilized in 0.5% (m/v) NaOH.

After this optimization, analyte signal reached to a reasonable value to decrease the sample concentration. For this reason, further studies were carried out with 1.0 mg/L sample solution prepared in a same way and also same experiment was repeated with this concentration. As can be seen from Figure 12, 6.0% (m/v) $NaBH_4$ gave the best results again.

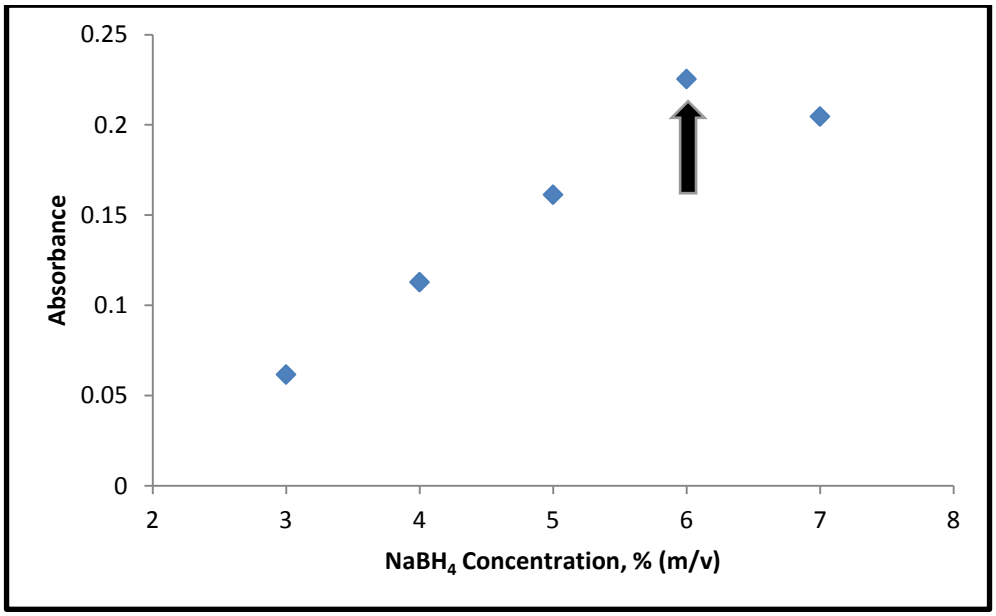

Figure 12 Effect of $NaBH_4$ concentration on the continuous flow VCGAAS signal of 1.0 mg/L Tl solution prepared in 0.5 mol/L HNO_3, 0.0005% (m/v) rhodamine B and 1.0 mg/L Pd. 50.0 mL/min Ar flow rate was used. Sample and $NaBH_4$ flow rates were set as 1.6 mL/min and 2.5 mL/min, respectively. $NaBH_4$ solutions were stabilized in 0.5% (m/v) NaOH.

3.1.4 Optimization of HNO_3 Concentration

Formation of volatile species strongly depends on HNO_3 concentration in the sample solution due to the fact that it affects pH of the reaction medium. 6.0%

(m/v) $NaBH_4$ was prepared in 0.5% (m/v) NaOH and mixed with sample solution through reaction and stripping coils. HNO_3 concentration of sample solution was varied between 0.3 mol/L and 2.0 mol/L. It was indicated in Figure 13 that 0.5 mol/L HNO_3 was optimum concentration for the acidity. However, Tl volatile species are unstable and decompose rapidly. That behavior is a problem discussed in the literature many times **(Ebdon et al., 1995; Zhu et al., 2000)**. During the studies, Tl volatile species were decomposed and formed black precipitates in the system. These black precipitates were adsorbed onto especially the reaction and stripping coils. Saturation of the system with Tl black precipitates lead to enhancement of signals. On the other hand, a serious memory effect problem was also encountered. While taking signals in higher acid concentrations, it was observed that the degree of saturation on the reaction and stripping coils with black precipitates decreased in a considerable amount. For this reason it was difficult to decide about the optimum acidity concentration. Consequently, it was not certain whether that signal decrease resulted from high acid of the sample solution or due to the saturation loss on the coils.

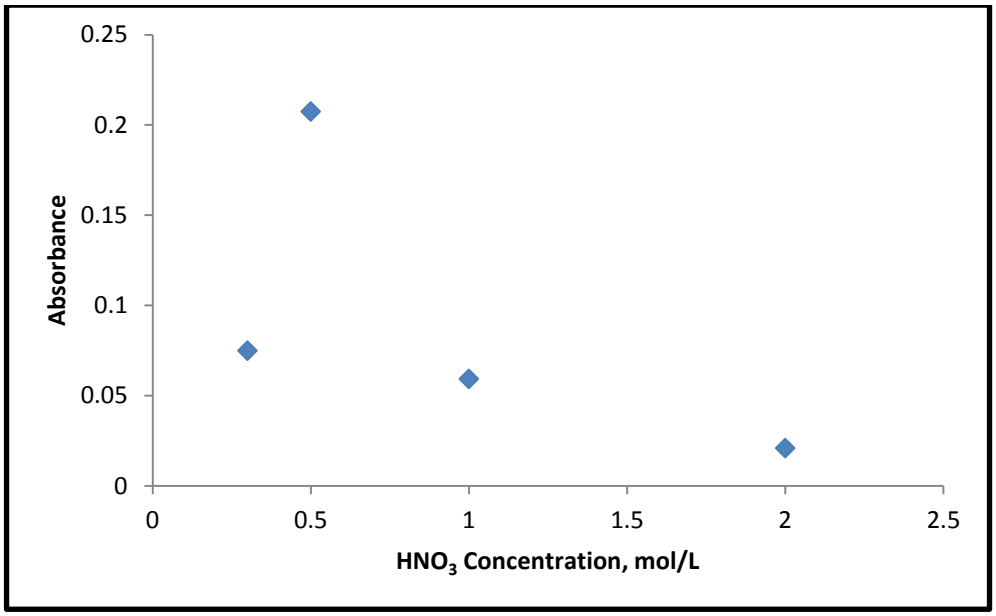

Figure 13 Effect of HNO_3 concentration on the continuous flow VCGAAS signal of 1.0 mg/L Tl solution prepared in 0.0005% (m/v) rhodamine B and 1.0 mg/L Pd. 50.0 mL/min Ar flow rate was used. 6.0% (m/v) $NaBH_4$ solution was stabilized in 0.5% (m/v) NaOH. $NaBH_4$ and acidified sample solution were sent with the flow rates of 2.5 mL/min and 1.6 mL/min, respectively.

3.1.5 Results from Continuous Flow VCG System

Due to unstable Tl volatile species, black precipitates in the coils and adsorptions on the dead volume of the GLS caused serious memory problems. In the course of HNO_3 optimization, black precipitates changed their locations erratically. Changes in the system saturation affected the signals and resulted in considerable decrease in the absorbance values. As a result, reproducibility and sensitivity of the method were lost and further optimizations could not be carried out. Parameters of the continuous flow VCGAAS system which could be optimized were summarized in Table 4.

Table 4 Optimized parameters for continuous flow volatile compound generation system.

Parameter	Optimum Value
$NaBH_4$ flow rate	2.5 mL/min
Sample flow rate	1.6 mL/min
Ar flow rate	50.0 mL/min
$NaBH_4$ concentration	6.0% (m/v)

3.2 Flow Injection Volatile Compound Generation System

In this part of the study, Tl volatile species are generated in flow injection mode and parameters were optimized to increase sensitivity.

3.2.1 Optimization of Ar Flow Rate

Flow injection VCG studies were carried out with 1.0 mg/L Tl solution. Sample solution and carrier solution were acidified with HCl to get a final concentration of 0.5 mol/L HCl. Rhodamine B and Pd were added to the sample solution to a final concentration of 0.0005% (m/v) and 1.0 mg/L, respectively. Sample was introduced to the system by the help of 100 µL sample loop. 3.0% (m/v) $NaBH_4$ stabilized in 0.5% (m/v) NaOH was used as reductant solution. Carrier solution and $NaBH_4$ flow rates were set as 0.8 mL/min and kept constant during the experiment. Different Ar flow rates ranging from 10.0 mL/min to 300.0 mL/min were examined to see the

effects of flow rate on the signal shape and peak height (Figure 14). Signal decrease at higher flow rates was observed due to dilution effect of the gas. On the other hand, lower flow rates caused peaks to be distorted and tailed since the carrier flow was not strong enough to strip out the volatile species effectively. In addition, at lower flow rates water droplets were also observed in the 4.0 cm PTFE tubing used to connect exit the port of the GLS and the inlet arm of T-tube. Water droplets in the tubing affect system performance adversely and reduce signals. Considering the effects on sensitivity and peak shape, 50.0 mL/min Ar flow rate was found as optimum.

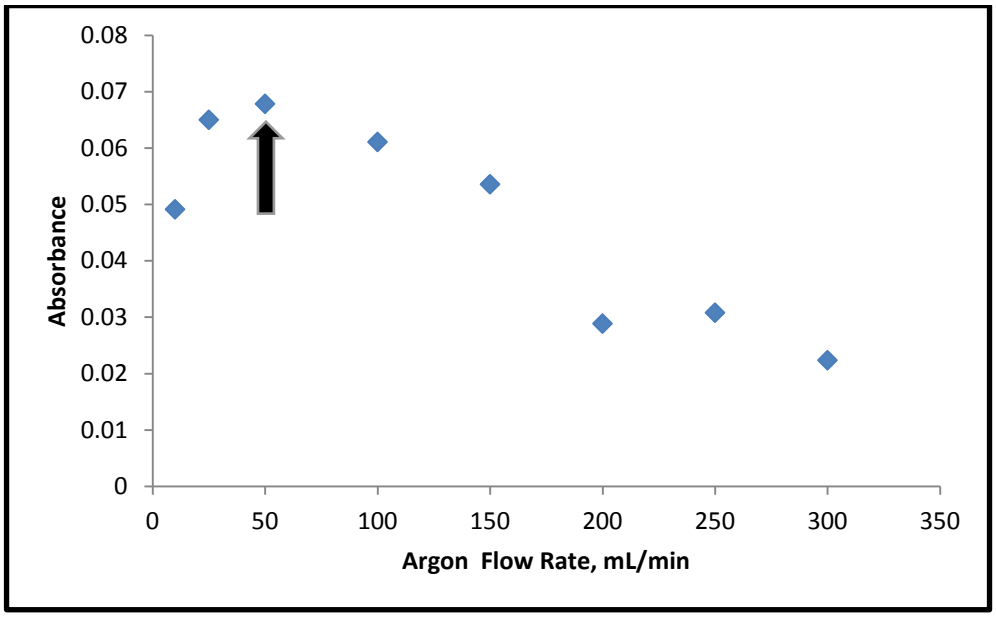

Figure 14 Effect of Ar flow rate on the flow injection VCGAAS signal of 1.0 mg/L Tl solution prepared in 0.5 mol/L HCl, 0.0005% (m/v) rhodamine B and 1.0 mg/L Pd. Carrier solution and 3.0% (m/v) $NaBH_4$ stabilized in 0.5% (m/v) NaOH were sent with the flow rate of 0.8 mL/min. 100 µL loop volume was used for sample introduction.

3.2.2 Optimization of $NaBH_4$ and HCl Concentrations

VCG reaction conditions and system performance strongly depend on reductant and acid concentrations used. Small changes in these concentrations affect pH of the reaction medium and hydrogen radical concentration; these changes may lead to significant differences in the analytical signals. HCl concentration of sample solution and carrier solution were varied between 0.1 mol/L and 2.0 mol/L. $NaBH_4$ solutions ranging from 1.0% (m/v) to 3.0% (m/v) were stabilized in 0.5% (m/v) NaOH. 100 µL loop volume was used to introduce the sample to the system. Reductant and carrier solution were sent with the flow rate of 0.8 mL/min. The results obtained from the optimization of $NaBH_4$ and HCl concentrations are given in Figure 15. Considering the peak shapes and reproducibility of the analytical signals, 0.5 mol/L HCl and 3.0% (m/v) $NaBH_4$ were chosen for further experiments; even though, a slightly higher absorbance value was obtained from 0.3 mol/L HCl and 3.0% (m/v) $NaBH_4$.

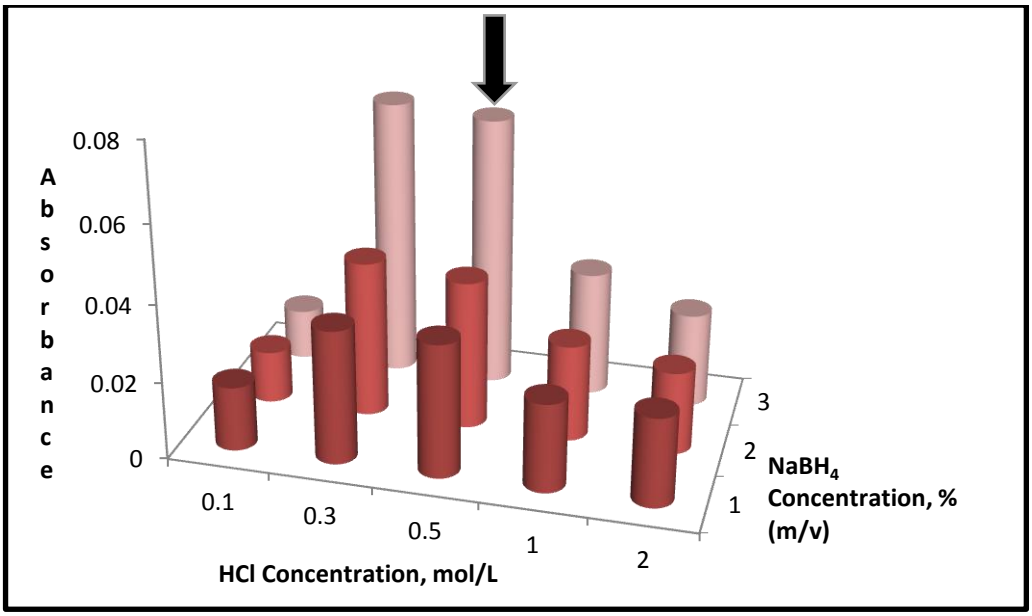

Figure 15 Effect of $NaBH_4$ and HCl concentrations on the flow injection VCGAAS signal of 1.0 mg/L Tl solution prepared in 0.0005% (m/v) rhodamine B and 1.0 mg/L Pd. Carrier solution and $NaBH_4$ were sent with the flow rate of 0.8 mL/min. 100 µL loop volume was used for sample introduction and Ar flow rate was 50.0 mL/min. $NaBH_4$ solution was stabilized in 0.5% (m/v) NaOH.

The effects of $NaBH_4$ concentrations higher than 3.0% (m/v) on VCG efficiency were also investigated (Figure 16). 0.5 mol/L HCl was used for sample solution and carrier solution, and $NaBH_4$ solutions ranging from 1.0% (m/v) to 8.0% (m/v) were prepared. 400 µL loop volume was used for the introduction of sample solution. Flow rates of carrier solution and $NaBH_4$ were adjusted to 1.0 mL/min. Although absorbance value was increasing together with $NaBH_4$ concentration up to 6.0% (m/v) in continuous flow system, there was no difference in absorbance values from 3.0% to 8.0% in flow injection system.

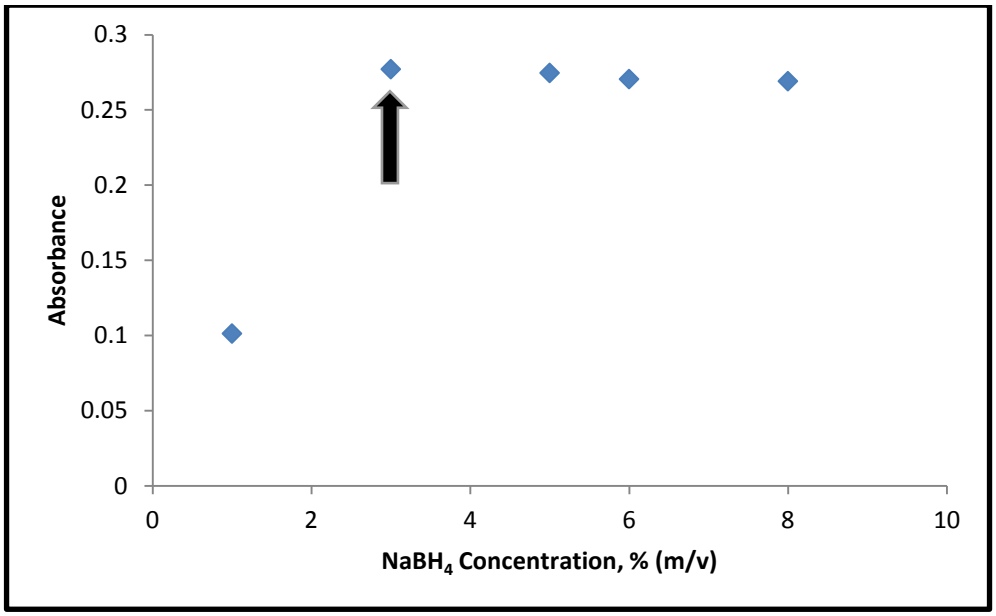

Figure 16 Effect of $NaBH_4$ on the flow injection VCGAAS signal of 1.0 mg/L Tl solution prepared in 0.0005% (m/v) rhodamine B, 0.5 mol/L HCl and 1.0 mg/L Pd. Carrier solution and $NaBH_4$ were sent with the flow rate of 0.8 mL/min. 400 µL loop volume was used for sample introduction and Ar flow rate was set as 50.0 mL/min. $NaBH_4$ solution was stabilized in 0.5% (m/v) NaOH.

3.2.3 Optimization of $NaBH_4$ and Carrier Solution Flow Rates

$NaBH_4$ and carrier solution were pumped with different flow rates ranging 0.8 mL/min to 1.3 mL/min by the help of peristaltic pumps. Results given in Figure 17 demonstrated that analytical signal increased with increasing flow rates. Because of the fact that small GLS with the volume of 3.0 mL was used for the flow injection VCG of Tl as distinct from conventional VCG systems, higher flow rates caused overflow of the GLS. In addition, water droplets on the PTFE tubing connected to the exit point of GLS were noticed at higher flow rates. In order to prevent

overflows of the GLS and water droplets on the tubing, 1.0 mL/min flow rate was accepted as optimum for $NaBH_4$ and carrier solutions.

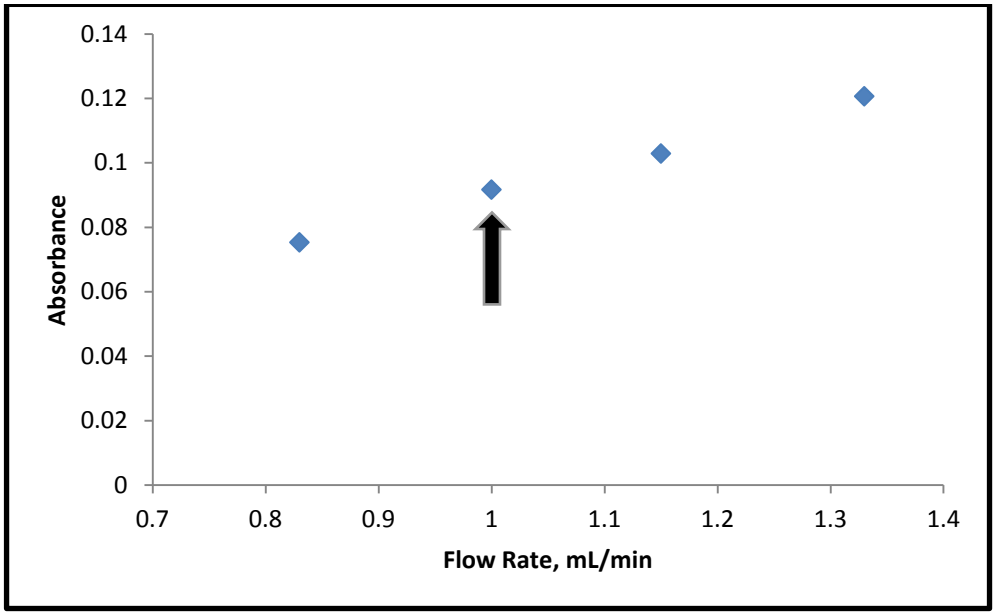

Figure 17 Effect of $NaBH_4$ and carrier solution flow rates on the flow injection VCGAAS signal of 1.0 mg/L Tl solution prepared in 0.0005% (m/v) rhodamine B, 0.5 mol/L HCl and 1.0 mg/L Pd. 3.0% (m/v) $NaBH_4$ stabilized in 0.5% (m/v) NaOH was used. 100 µL loop volume was used for sample introduction and Ar flow rate was 50.0 mL/min.

3.2.4 Optimization of Rhodamine B Concentration

Rhodamine B which is an alkaline dye has been widely used for the determination of Tl by VCG. It has been proven that as a co-enhancement reagent rhodamine B increases peak height of analytical signal in the presence of Pd **(Xu, Zhou, Du, & Zhu, 2001)**. Sample solution was prepared in 0.5 mol/L HCl, 1.0 mg/L Pd and rhodamine B. The concentration of rhodamine B was varied from 0.0005% (m/v) to

0.01% (m/v) to see the effects on the peak height. According to experimental results given in Figure 18, 0.005% (m/v) rhodamine B in the presence of 1.0 mg/L Pd showed the best performance for enhancing VCG efficiency of Tl.

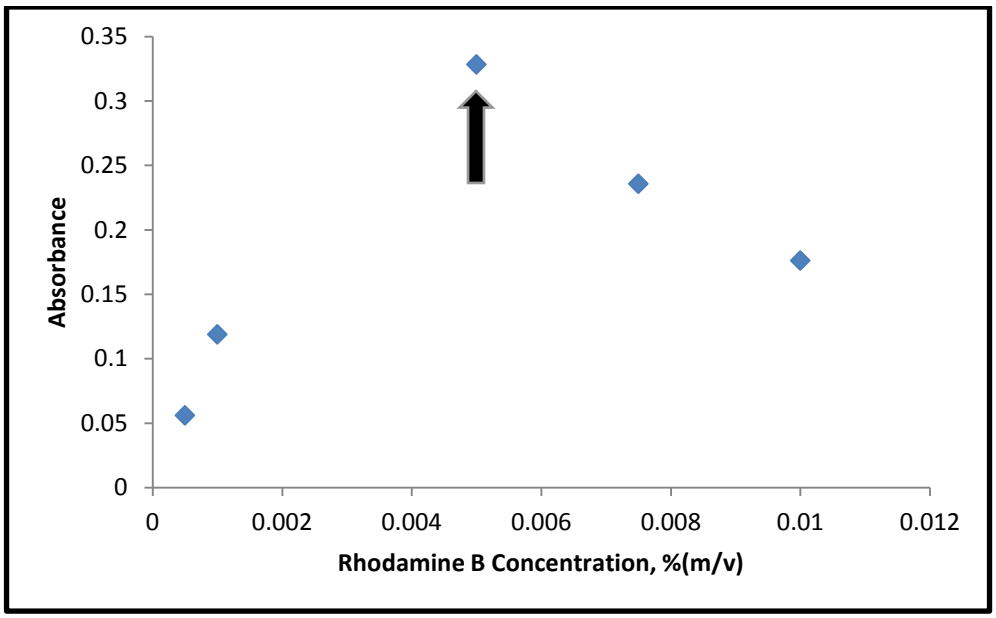

Figure 18 Effect of rhodamine B concentration on the flow injection VCGAAS signal of 1.0 mg/L Tl solution prepared in 0.5 mol/L HCl and 1.0 mg/L Pd. Carrier solution and 3.0% (m/v) $NaBH_4$ stabilized in 0.5% (m/v) NaOH were sent with the flow rate of 1.0 mL/min. 100 µL loop volume was used for sample introduction and Ar flow rate was 50.0 mL/min.

In the optimization of rhodamine B concentration with 100 µL sample loop, no signal was obtained from the sample solution prepared in the absence of rhodamine B and Pd. After that, loop volume was increased to 400 µL and experiment was repeated in the same conditions (Figure 19). Analytical signal obtained from 1.0 mg/L Tl prepared in 0.5 mol/L HCl can be seen in curve b in Figure 19. It was proved that 100 µL sample loop remained inadequate to obtain a

meaningful signal from the sample that did not contain rhodamine B and Pd. On the other hand, presence of 0.005% (m/v) rhodamine B and 1.0 mol/L Pd hastened the reaction and enhanced the peak height of the signal as can be seen from the curve a. Peak-shaped and intense signal was obtained in a shorter time.

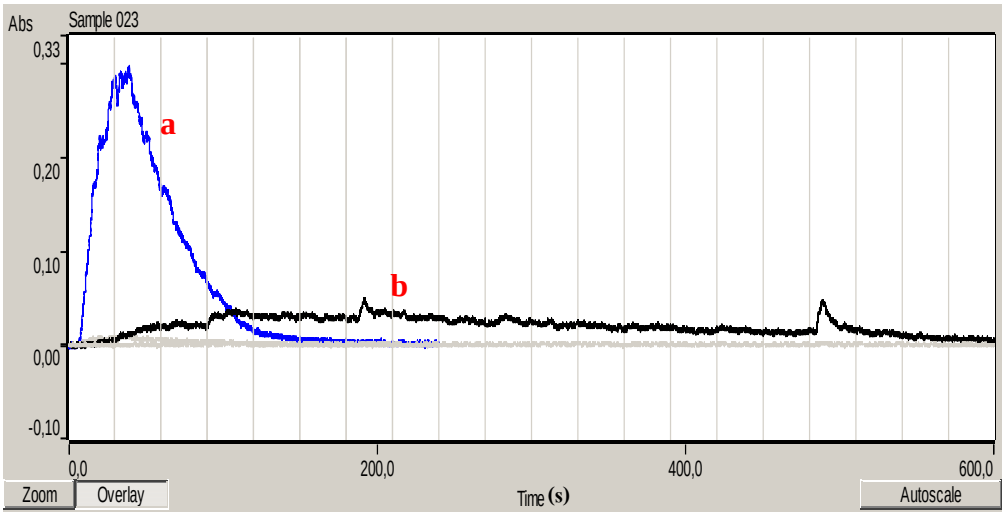

Figure 19 a- Analytical signal obtained from 1.0 mg/L Tl prepared in 0.5 mol/L HCl, 0.005% (m/v) rhodamine B and 1.0 mg/L Pd. **b-** Analytical signal obtained from 1.0 mg/L Tl prepared in 0.5 mol/L HCl. 400 µL loop volume was used for sample introduction.

3.2.5 Optimization of Sample Loop Volume

In flow injection VCG system, sample in the sample loop was introduced to the system by the help of a manual injection valve. Optimization of sample loop volume is important because it affects analyte atom concentration in the measurement zone. As can be seen from Figure 20, different loop volumes ranging 100 µL to 800 µL were examined. It was observed that there was a slight difference on absorbance values obtained using 400 µL and 800 µL loop volumes. Considering reagent

consumption and sensitivity, 400 µL sample loop volume was chosen for further experiments.

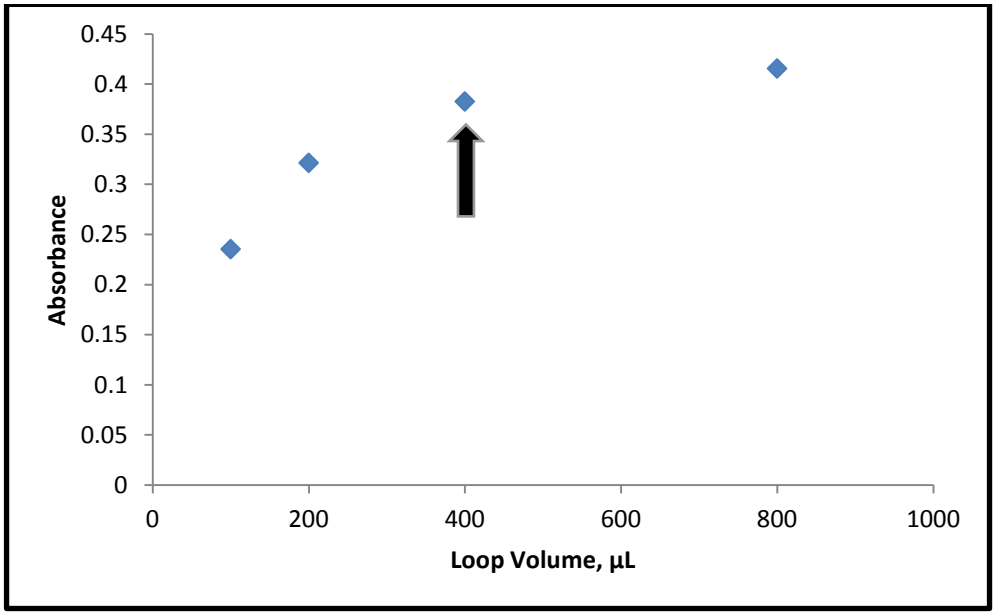

Figure 20 Effect of sample loop volume on the flow injection VCGAAS signal of 1.0 mg/L Tl solution prepared in 0.5 mol/L HCl, 0.005% (m/v) rhodamine B and 1.0 mg/L Pd. Carrier solution and 3.0% (m/v) $NaBH_4$ stabilized in 0.5% (m/v) NaOH were sent with the flow rate of 1.0 mL/min. Ar flow rate was 50.0 mL/min.

3.2.6 Effect of HCl and HNO_3 on VCG Efficiency of Tl^+ and Tl^{3+}

Considering toxic effects on human health and environment, determination of Tl at lower detection limits is very important. However, in literature, there is no agreement on the type of the acid which provides a better performance in the determination of Tl. Liao et al. **(Liao, Chen, Yan, Li, & Ni, 1998)** used HCl for the investigation of Tl VCG using in situ trapping in graphite tube by AAS. On the other hand, Zhu et al. **(Zhu & Xu, 2000)** recommended using HNO_3 for VCG of Tl since

formation of Tl-Cl complex in HCl medium caused unstable signals and reduction in sensitivity. For this reason, the effects of different acids on the VCG efficiency of Tl in different oxidation states were investigated. HCl and HNO_3 were selected to acidify the carrier solution and sample solutions of Tl^{+} and Tl^{3+}. Acidified sample solutions were prepared in the presence of rhodamine B and Pd with the final concentrations of 0.005% (m/v) and 1.0 mg/L, respectively. Absorbance values obtained from Tl^{+} species can be seen from Figure 21. It was clear that VCG efficiency of Tl^{+} species was increasing in the presence of HNO_3 and signals of HCl solutions were more noisy and unstable.

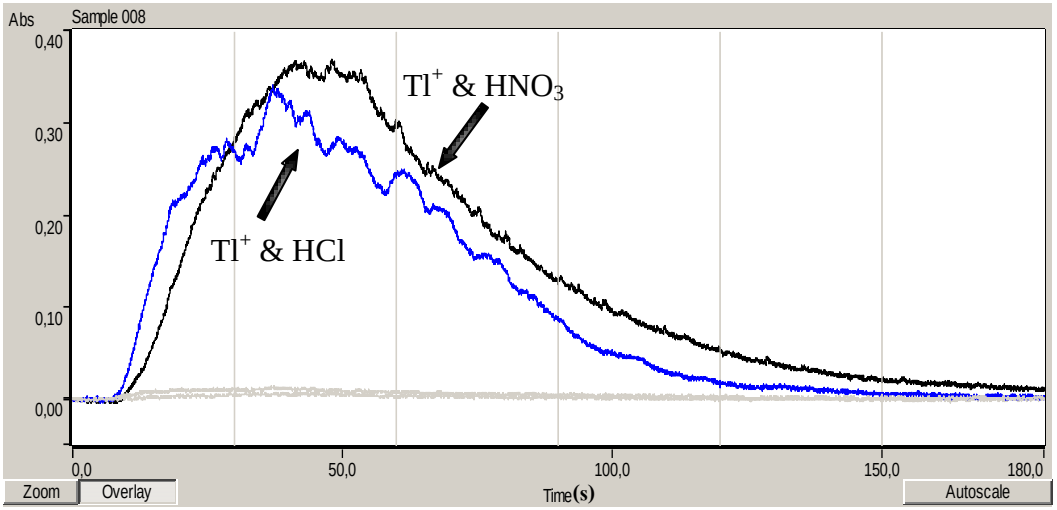

Figure 21 Effects of HNO_3 and HCl on the shape of VCGAAS signal of 1.0 mg/L Tl^{+} solution prepared in 0.005% (m/v) rhodamine B and 1.0 mg/L Pd. Acidity of the sample and carrier solution were 0.5 mol/L. Carrier solution and 3.0% (m/v) $NaBH_4$ stabilized in 0.5% (m/v) NaOH were sent with the flow rate of 1.0 mL/min. Ar flow rate was 50.0 mL/min and 400 µL loop volume was used for sample introduction.

VCG efficiency of Tl^{+3} species also have been affected significantly by the type of the acid used (Figure 22). Although, nearly the same absorbance values were obtained

from Tl^{3+} and Tl^{+} species in the presence of HNO_3, using HCl caused a significant decrease in the signals of Tl^{3+} species. Fluctuations and excess noise in the analytical signals were important problems in HCl medium.

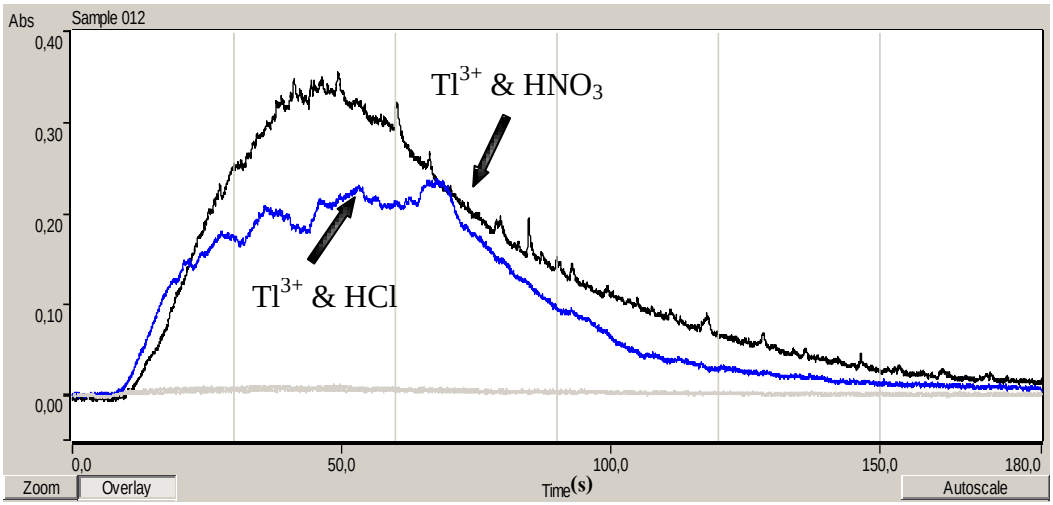

Figure 22 Effects of HNO_3 and HCl on the shape of VCGAAS signal of 1.0 mg/L Tl^{3+} solution prepared in 0.005% (m/v) rhodamine B and 1.0 mg/L Pd. Acidity of the sample and carrier solution were 0.5 mol/L. Carrier solution and 3.0% (m/v) $NaBH_4$ stabilized in 0.5% (m/v) NaOH were sent with the flow rate of 1.0 mL/min. Ar flow rate was 50.0 mL/min and 400 µL loop volume was used for sample introduction.

In spite of the fact that HNO_3 provided a better performance for both oxidation states of Tl, sample solutions prepared in HCl remained stable for longer times. As can be seen Figure 23-a, sample solutions containing rhodamine B were observed to decompose even after a day in the presence of HNO_3. Decomposition process was faster when the solutions were subjected to sunlight and black precipitates were observed in HNO_3 solutions after about a month (Figure 23-b).

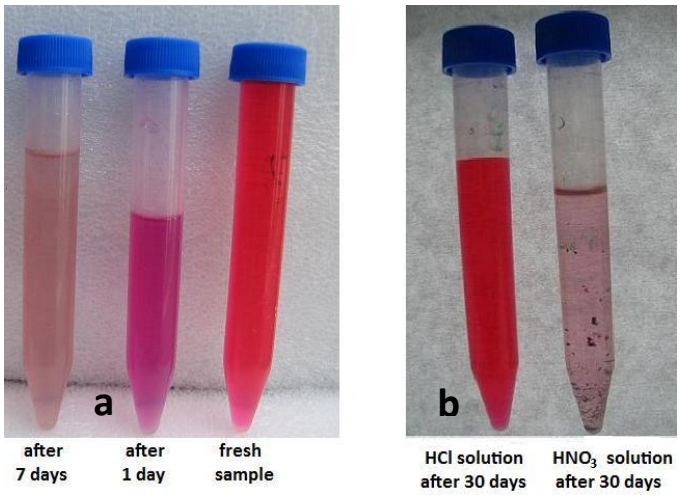

Figure 23 a- Decomposition process of sample solution prepared in HNO_3. **b-** Sample solutions prepared in HCl and HNO_3 after 30 days passed.

As a result, VCG efficiency of Tl^+ species was higher in both HCl and HNO_3. Analytical signals obtained from Tl^+ and Tl^{3+} solutions prepared in HNO_3 were less noisy and had better peak shapes. For this reason, Tl^+ solutions in the presence of HNO_3 were used as sample solutions for further studies and prepared daily prior to usage.

3.2.7 Effects of Enhancement Reagents

Compared to other volatile compound forming elements, low sensitivity of Tl volatile species has been reported in the literature many times and using an appropriate enhancement reagent is advised. Enhancement effects of Pd and Te on the signals of volatile Tl species attract attention in recent studies. For this reason, Pd and Te concentrations in the sample solutions were optimized and effects on the peak height of the signals were compared.

1.0 mg/L Tl^+ solutions were prepared in the presence of HNO_3 and rhodamine B to get final concentrations of 0.5 mol/L and 0.005% (m/v), respectively. Pd concentration in the sample solution was varied between 1.0 mg/L and 5.0 mg/L. Sample solution in the absence of Pd was also examined. Results given in Figure 24 implied that presence of 1.0 mg/L Pd in the sample solution enhanced the analytical signal significantly.

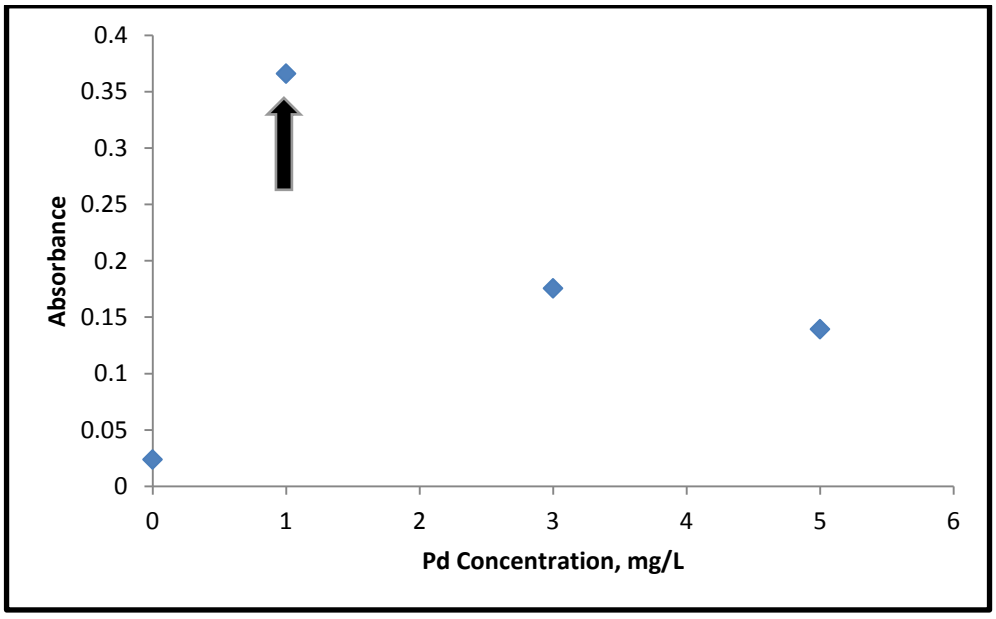

Figure 24 Effects of Pd concentration on the flow injection VCGAAS signal of 1.0 mg/L Tl^+ solution prepared in 0.5 mol/L HNO_3, 0.005% and (m/v) rhodamine B. Carrier solution and 3.0% (m/v) $NaBH_4$ stabilized in 0.5% (m/v) NaOH were sent with the flow rate of 1.0 mL/min. Ar flow rate was 50.0 mL/min and 400 µL loop volume was used for sample introduction.

The concentration of Te was altered from 1.0 mg/L to 15.0 mg/L in the optimization process. As can be seen Figure 25, there was no difference in absorbance values

between 8.0 mg/L and 15.0 mg/L. So as to reduce reagent consumption, 8.0 mg/L Te was selected as optimum.

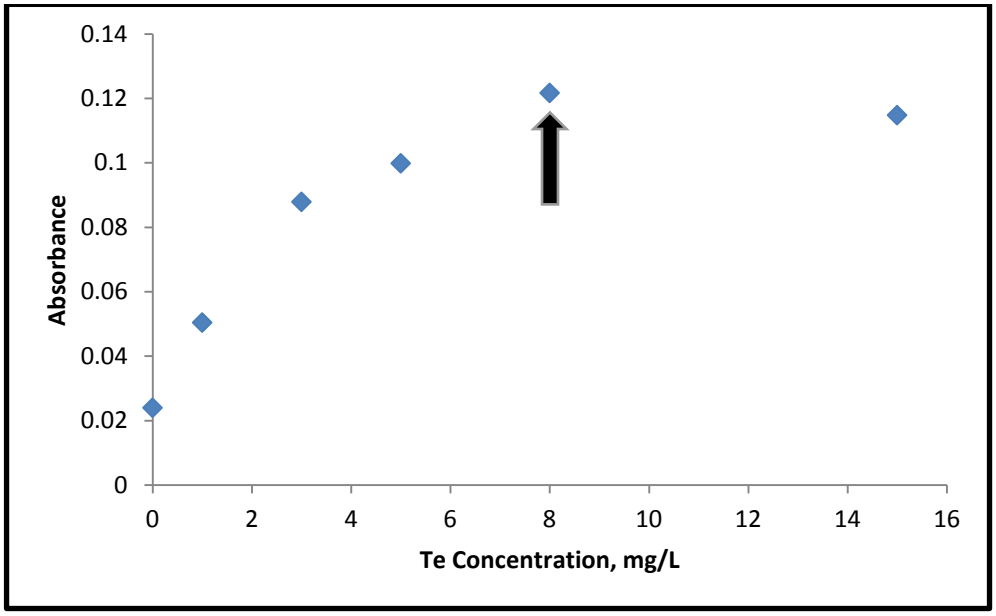

Figure 25 Effects of Te concentration on the flow injection VCGAAS signal of 1.0 mg/L Tl^{+} solution prepared in 0.5 mol/L HNO_3, 0.005% and (m/v) rhodamine B. Carrier solution and 3.0% (m/v) $NaBH_4$ stabilized in 0.5% (m/v) NaOH were sent with the flow rate of 1.0 mL/min. Ar flow rate was 50.0 mL/min and 400 µL loop volume was used for sample introduction.

Experimental results shown in Figure 26 indicated that enhancement factor of 1.0 mg/L Pd on the peak height of the signal was about 3 times higher than the 8.0 mg/L Te. Sensitivity improvement and reagent consumption were taken into consideration and Pd provided the best performance for VCG of Tl and it was chosen as the enhancement reagent.

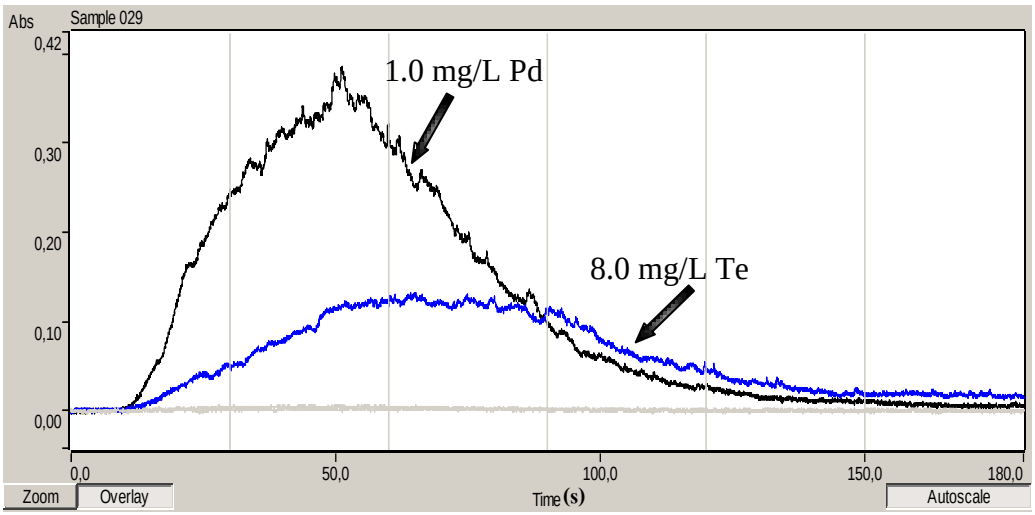

Figure 26 Effects of 1.0 mg/L Pd and 8.0 mg/L Te on the shape of VGCAAS signal of 1.0 mg/L Tl^{+} solution prepared in 0.5 mol/L HNO_3 and 0.005% (m/v) rhodamine B. Carrier solution and 3.0% (m/v) $NaBH_4$ stabilized in 0.5% (m/v) NaOH were sent with the flow rate of 1.0 mL/min. Ar flow rate was set as 50.0 mL/min and 400 µL loop volume was used for sample introduction.

3.2.8 Linear Ranges and Calibration Plots

After all optimization studies were completed, analytical signals of Tl^{+} solutions ranging from 0.1 mg/L to 5.0 mg/L were measured to determine the linear dynamic range and calibration plot for HNO_3 and HCl (Figure 27). Each data point is the mean of three replicate measurements.

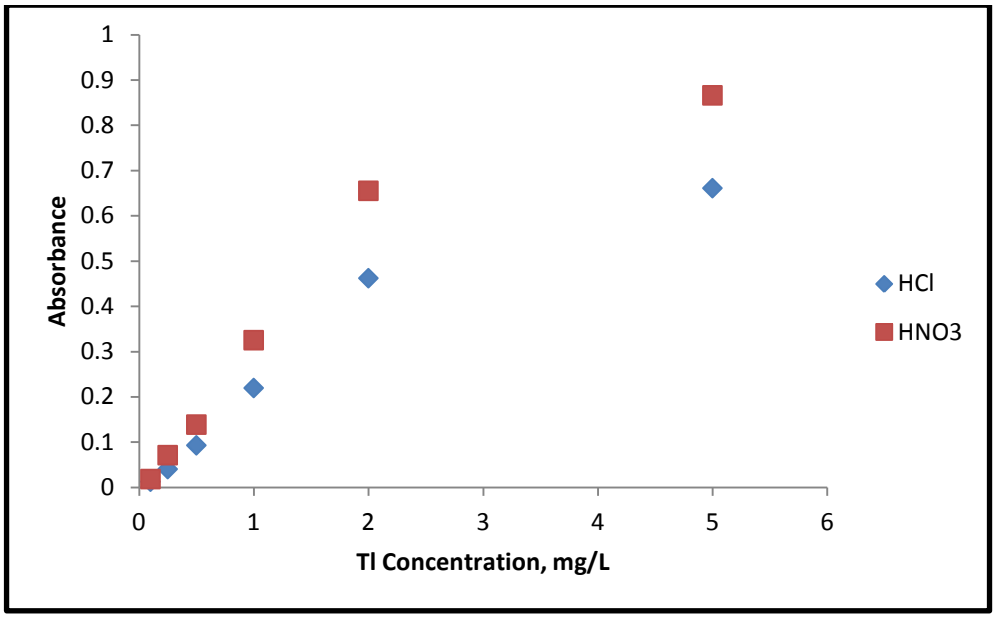

Figure 27 Calibration data in 0.5 mol/L HNO_3 and 0.5 mol/L HCl for the flow injection VCGAAS signal of 1.0 mg/L Tl^+ solution prepared in 0.005% (m/v) rhodamine B and 1.0 mg/L Pd. Carrier solution and 3.0% (m/v) $NaBH_4$ stabilized in 0.5% (m/v) NaOH were sent with the flow rate of 1.0 mL/min. Ar flow rate was set as 50.0 mL/min and 400 µL loop volume was used for sample introduction.

It was observed that for the media using both acids the plot was linear between 0.1 mg/L and 2.0 mg/L Tl^+. After this point, deviation from linearity was observed (Figure 27). LOD and LOQ values were calculated from the standard deviation of 6 replicate measurements of the standard with lowest concentration of 0.1 mg/L. For the calculation of characteristic concentration, absorbance value of 1.0 mg/L standard was used. Linear portions of the calibration plots are shown in Figure 28. Analytical figures of merit for flow injection VCGAAS are given in Table 5.

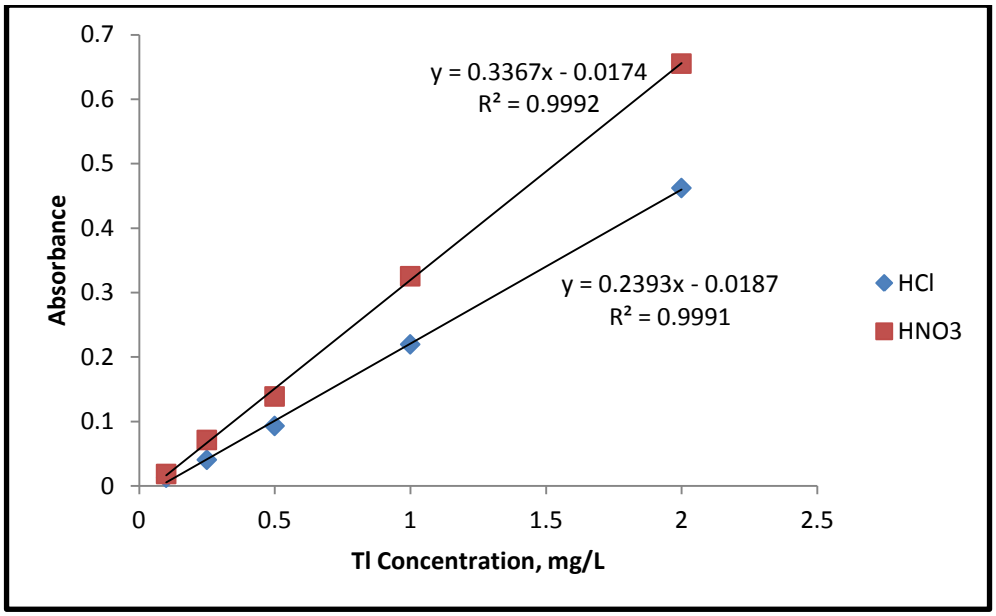

Figure 28 Linear portions of calibration plots in 0.5 mol/L HNO_3 and 0.5 mol/L HCl for the flow injection VCGAAS signal of 1.0 mg/L Tl^+ solution prepared in 0.005% (m/v) rhodamine B and 1.0 mg/L Pd. Carrier solution and 3.0% (m/v) $NaBH_4$ stabilized in 0.5% (m/v) NaOH were sent with the flow rate of 1.0 mL/min. Ar flow rate was 50.0 mL/min and 400 µL loop volume was used for sample introduction.

Table 5 Analytical figures of merit of flow injection VCGAAS system.

	Sample in the presence of HCl	**Sample in the presence of HNO_3**
Limit of Detection, LOD, 3s/m (N=6) ng/mL	14.0	12
Limit of Quantification, LOQ, 10s/m (N=6) ng/mL	45.0	40
Characteristic Concentration, C_0, ng/mL	19.9	13.4
Linear Range, mg/L	0.1 – 2.0	0.1 – 2.0
Relative Standard Deviation, RSD% (N=6)	8.6	7.2

The comparison between the results of this study and some studies from the literature are summarized in Table 6.

Table 6 The comparison of characteristic mass and characteristic concentrations of the studies.

Method	Characteristic Mass, ng	Characteristic concentration, ng/mL	Reference
VCGAAS	5.4	13.4	this study
Continuous flow HG		4	**(Ebdon, Goodal, Hill, Stockwell, & Thompson, 1995)**
In-situ trapping in graphite tube AAS	0.92		**(Liao, Chen, Yan, Li, & Ni, 1998)**
HGAAS	120		**(Yan, Yan, Cheng, & Li, 1984)**

Optimized parameters of flow injection VCGAAS system are summarized in Table 7.

Table 7 Optimized parameters of flow injection VCGAAS system.

Parameter	Optimum Value
Ar flow rate	50.0 mL/min
$NaBH_4$ concentration	3.0% (m/v) in 0.5% (m/v) NaOH
Acidity	0.5 mol/L HNO_3
$NaBH_4$ and carrier liquid flow rates	1.0 mL/min
Rhodamine B concentration	0.005% (m/v)
Sample loop volume	400 µL
Pd concentration	1.0 mg/L
OR	
Te concentration	8.0 mg/L

Enhancement factors of Pd and Te in the presence of rhodamine B is shown in Table 8. Significant enhancement factors were not obtained from sample solutions containing only rhodamine B, or Pd or Te.

Table 8 Characteristic concentrations and enhancement factors of Pd and Te.

Sample	C_0, ng/mL	Enhancement
1.0 mg/L Tl^+	125	1
1.0 mg/L Tl^+ 8.0 mg/L Te 0.005% (m/v) rhodamine B	34.5	3.6
1.0 mg/L Tl^+ 1.0 mg/L Pd 0.005% (m/v) rhodamine B	13.4	9.3

3.3 Reasons of Peak Broadening

In flow injection VCG system, 400 µL sample loop was used to introduce sample to the system and flow rate of carrier solution was set as 1.0 mL/min. The signal started about 10 seconds later from the injection. In that case the signal should have been completed in about 30 seconds. Analytical signal for 1.0 mg/L Tl^+ shown in Figure 29 demonstrates that it takes about 150 seconds to complete the signal. This is about five times longer than time required delivering the sample plug of the loop volume to the generator.

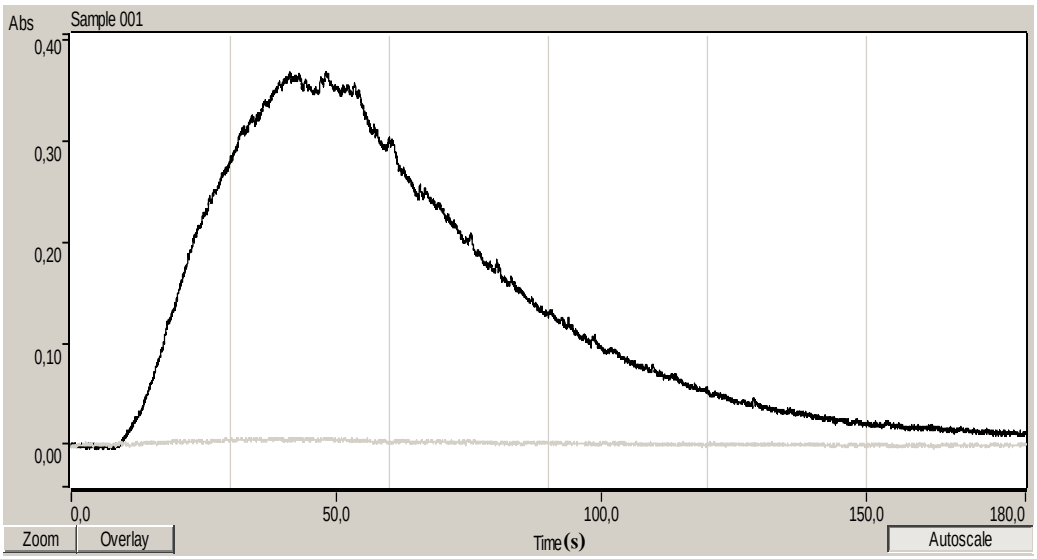

Figure 29 Analytical signal for 1.0 mg/L Tl^{+} solution prepared in 0.5 mol/L HNO_3, 0.005% (m/v) rhodamine B and 1.0 mg/L Pd. Carrier solution and 3.0% (m/v) $NaBH_4$ stabilized in 0.5% (m/v) NaOH were sent with the flow rate of 1.0 mL/min. Ar flow rate was set as 50.0 mL/min and 400 µL loop volume was used for sample introduction.

In order to understand reasons of peak broadening, a 3-way valve was introduced to the system. By this way, Ar was sent from either upstream or downstream of the GLS (Figure 30). In the experiment, GLS was bypassed by the flow of carrier gas in times 50 and 75 seconds using the downstream mode in this interval.

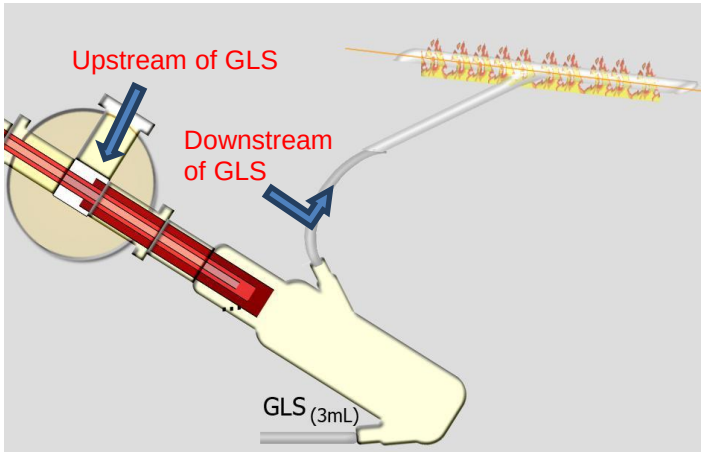

Figure 30 The positions of upstream and downstream of the GLS in flow injection VCG system.

Firstly, Ar was sent from the upstream of the GLS for 50 seconds. By the help of 3-way valve, the direction of the gas was changed immediately and it was sent from the downstream of the GLS. Ar flow from downstream resulted in decrease in the analytical signal (Figure 31). After 25 seconds, the direction of Ar was changed to upstream of the GLS again and increase in the analytical signal was observed. This experiment revealed that most of the memory effect causing peak broadening in the signals comes from the GLS or before the GLS. Moreover, in the time interval between 50 and 75 seconds, the signal did not decrease to the baseline level. That indicates that T-tube atomizer and/or connection tubings are also acting as some source of memory effect.

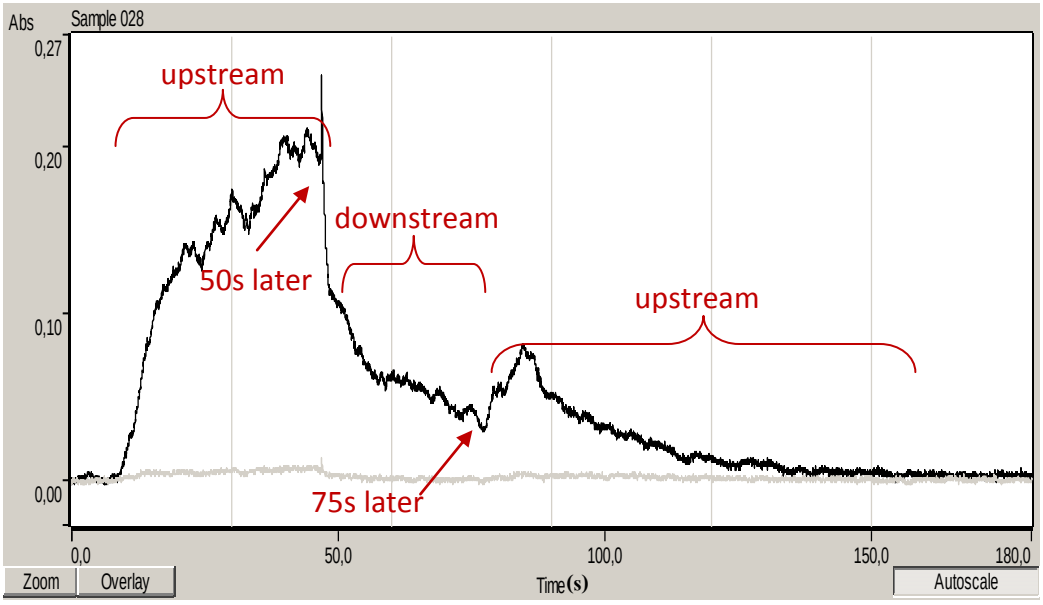

Figure 31 Effects of Ar sent from upstream and downstream of the GLS on the shape of VGCAAS signal of 1.0 mg/L Tl^{+} solution prepared in 0.5 mol/L HNO_3, 0.005% (m/v) rhodamine B and 1.0 mg/L Pd. Carrier solution and 3.0% (m/v) $NaBH_4$ stabilized in 0.5% (m/v) NaOH were sent with the flow rate of 1.0 mL/min. Ar flow rate was set as 50.0 mL/min and 400 µL loop volume was used for sample introduction.

3.4 Thallium Volatile Species

Unstability and fast decomposition of Tl volatile species is a problem that has been discussed in the literature many times. Black precipitates adsorbed on the system cause serious memory effects affecting system performance. So as to understand the behavior of Tl volatile species, a 0.2 µm-pore-size syringe filter was placed downstream of the GLS (Figure 32).

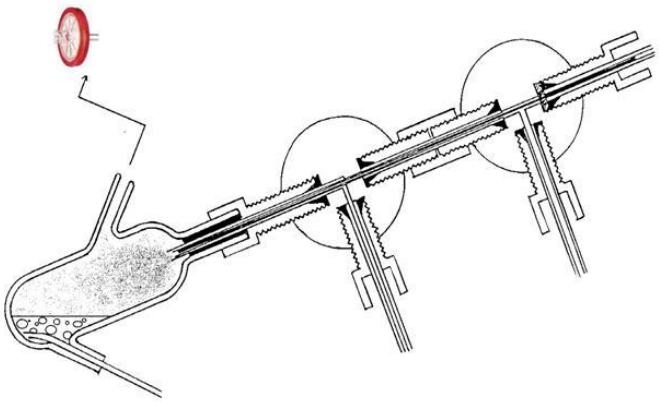

Figure 32 0.2 µm-pore-size syringe filter placed downstream of the GLS.

As can be seen from Figure 33, no signal was obtained in the presence of filter and this indicated that Tl volatile species were trapped on the filter. In order to compare the behavior of Tl volatile species with other volatile compound forming elements, Sb was chosen as another hydride forming analyte and the experiment was repeated in the same conditions. Analytical signal shown in Figure 34 proved that Sb volatile species were not trapped on the filter and they were transported to the atomizer.

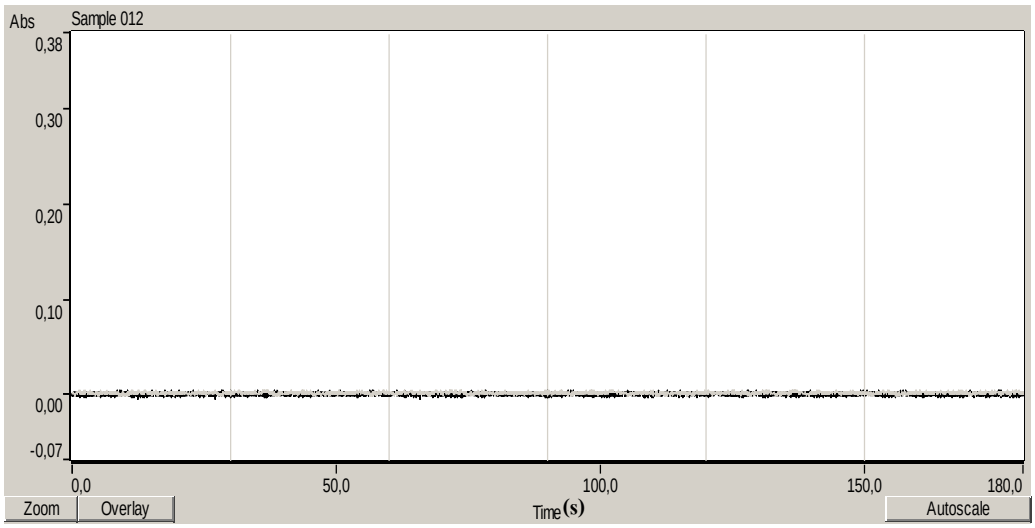

Figure 33 Analytical signal for 1.0 mg/L Tl^{+} solution prepared in 0.5 mol/L HCl, 0.005% (m/v) rhodamine B and 1.0 mg/L Pd when 0.2 µm-pore-size syringe filter placed downstream of the GLS. Conditions given on Table 6 were used.

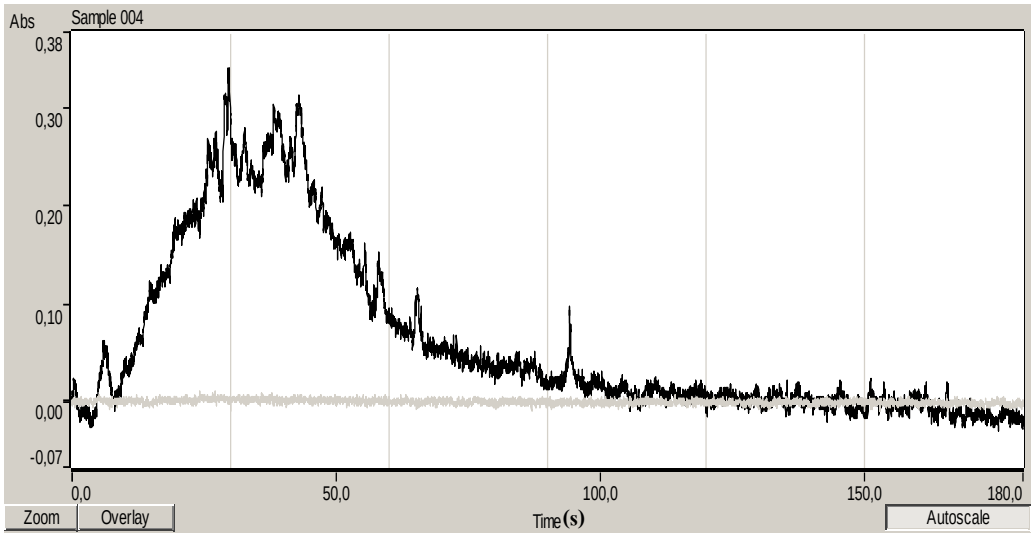

Figure 34 Analytical signal for 1.0 mg/L Sb solution prepared in 0.5 mol/L HCl when 0.2 µm-pore-size syringe filter placed downstream of the GLS. Carrier solution and 3.0% (m/v) $NaBH_4$ stabilized in 0.5% (m/v) NaOH were sent with the flow rate of 1.0 mL/min. Ar flow rate was 50.0 mL/min and 400 µL loop volume was used for sample introduction.

It is obvious that Tl volatile species shows a different behavior from other volatile compound forming elements. To further investigate the nature of these species, transmission electron microscope (TEM) and energy dispersive X-ray spectroscopy (EDS) microanalysis were employed. In the experiment, carbon/formvar coated Cu grids were placed downstream of the GLS to collect particles under optimized conditions. Tl volatile species were continuously generated from 10.0 mg/L Tl solutions and transported to the grids. Volatile species were collected for 80 seconds and the grids were allowed to dry at ambient conditions waited for drying on their own. The samples were examined in TEM and the image shown in Figure 35 demonstrates that Tl is generated in the form of nanoparticles. EDS spectrum proved the presence of Tl and also Pd at the surface of grids (Figure 36).

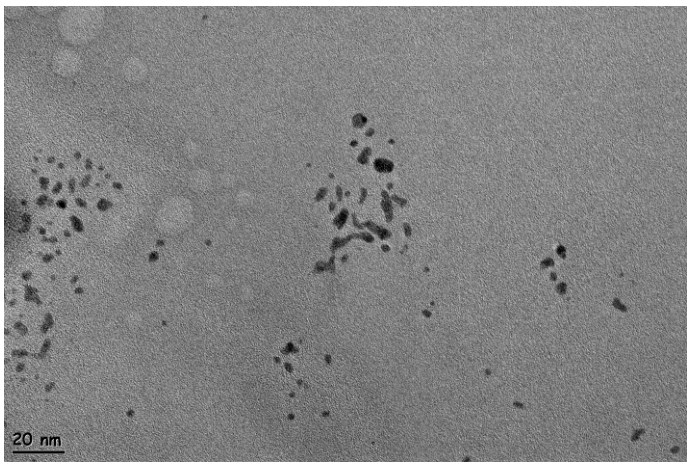

Figure 35 TEM image of thallium nanoparticles adsorbed onto carbon coated formvar film.

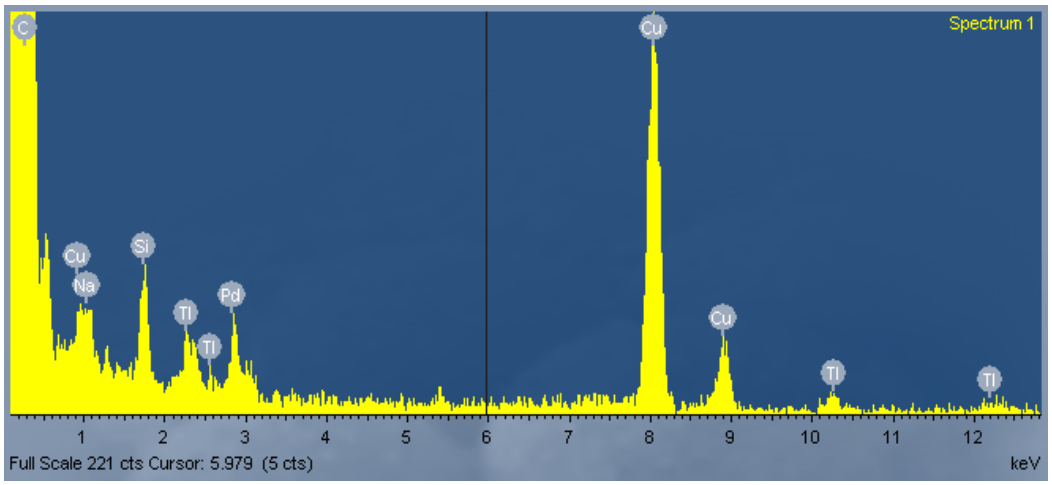

Figure 36 EDS spectrum of thallium nanoparticles adsorbed onto carbon coated formvar film.

The particle shown in Figure 37 has a diameter of about 20 nm and EDS spectrum of this particle (Figure 38) supports the idea that it is a Tl nanoparticle. The intensive Cu peak comes from the grid material. The proof, that it is a Tl nanoparticle, is presented in Figure 39 showing EDS spectrum of background, obtained by using the grid before the experiment involving Tl. In the background spectrum, there are no peaks corresponding to Tl.

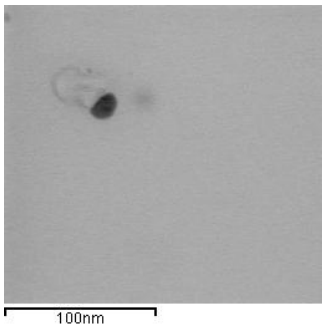

Figure 37 TEM image of about 20 nm particle size thallium nanoparticle adsorbed onto carbon formvar film.

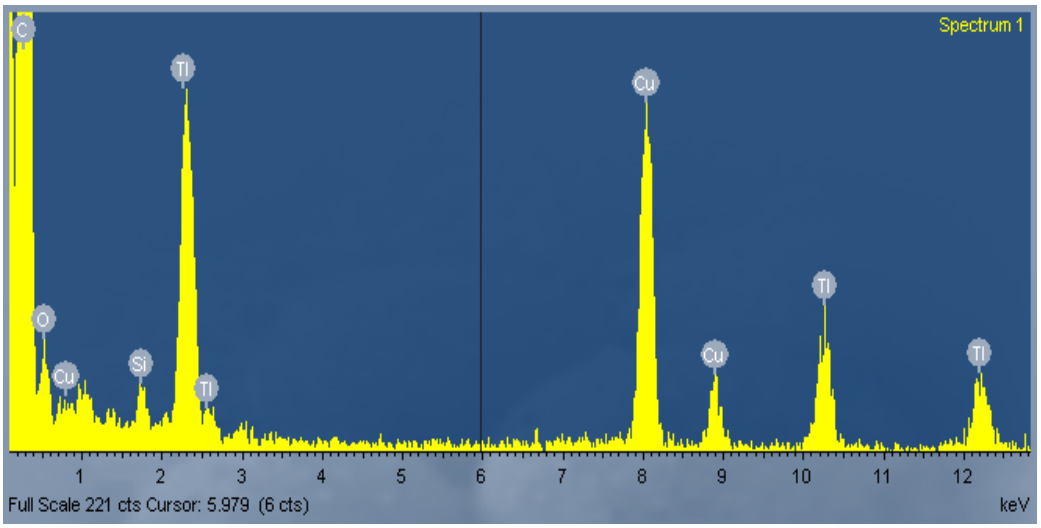

Figure 38 EDS spectrum of about 20 nm particle size thallium nanoparticle adsorbed onto carbon formvar film.

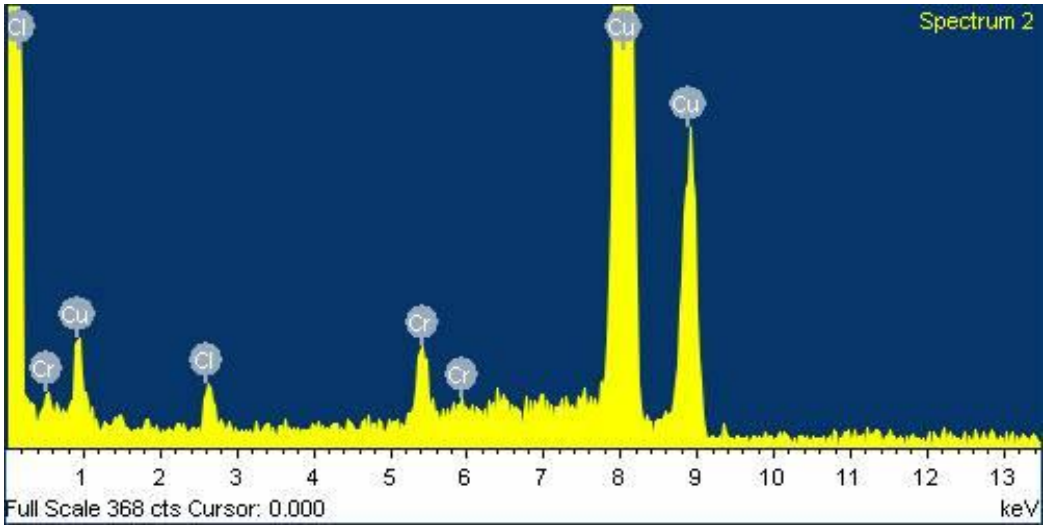

Figure 39 EDS spectrum of background

CHAPTER 4

CONCLUSIONS

The main purpose of this study was the development of a sensitive analytical method for the determination of thallium at low detection limits and to investigate the nature of transportable thallium species.

The first part of the study involves determination of thallium by continuous flow volatile compound generation AAS system. In this part $NaBH_4$, sample and Ar flow rates, $NaBH_4$ and HNO_3 concentrations were optimized. 50.0 mL/min Ar flow rate found as optimum because of dilution effect of the higher flow rates and 6.0% (m/v) $NaBH_4$ enabled rapid and efficient formation of volatile species. During the optimizations, black precipitates were observed in the reaction and stripping coils. Adsorptions on the dead volume of the GLS and black precipitates in the tubings caused serious memory problems. In the optimization of HNO_3 concentration, changes in the degree of the saturation of the system caused sensitivity loss and further development could not be done.

Second part of the study involves determination of thallium by a special flow injection volatile compound generation AAS system. The most important feature of this system was that it was based on fast separation of gaseous phase from the solution. This feature enabled reducing most of the memory effect. 0.5 mol/L acidity and 3.0% (m/v) for $NaBH_4$ concentration were effective in increasing the analytical signal. In addition, 0.005% (m/v) rhodamine B in the presence of 1.0 mg/L

Pd hastened the reaction and enhanced peak height of the analytical signal. Type of the acid used was affected peak height and peak shapes of the signals obtained from Tl^{+} and Tl^{3+} species.

Third part deals with the reasons of peak broadening in the signals. The sources of memory effects causing peak broadening in the signals were investigated by changing the location of introduction for the Ar. It was found that, most of the memory effect was coming from the GLS or before the GLS. T-tube atomizer was also some source of memory.

The last part of the study was a search for the nature and behavior of the Tl volatile species. It was shown that when a filter was placed in the system, no absorbance value was obtained from Tl volatile species which were trapped on the filter. According to TEM and EDS results, Tl and also Pd nanoparticles were retained on the carbon/formvar coated Cu grids.

REFERENCES

Anderson, J. R. (1953). Detection and Determination of Thallium. *Anal. Chem. , 25*, 108-112.

Arbab-Zavar, M. H., Chamsaz, M., Yousefi, A., & Ashraf, N. (2009). Electrochemical Hydride Generation of Thallium. *Talanta , 79*, 302-307.

Arslan, Y., Matoušek, T., Kratzer, J., Musil, S., Benada, O., Vobecký, M., et al. (2011). Gold Volatile Compound Generation: Optimization, Efficiency and Characterization of the Generated Form. *J. Anal. At. Spectrom. , 26*, 828-837.

Asami, T., Mizui, C., Shimada, T., & Kubota, M. (1996). Determination of Thallium in Solids by Flame Atomic Absorption Spectrometry. *Fresen. J. Anal. Chem. , 356*, 348-351.

Ataman, O. Y. (2008). Vapor Generation and Atom Traps: Atomic Absorption Spectrometry at the ng/L Level. *Spectrochim. Acta, Part B , 63*, 825-834.

Bakırdere, S., Aydın, F., Bakırdere, E. G., Titretir, S., Akdeniz, İ., Aydın, I., et al. (2011). From mg/kg to pg/kg Levels: A Story of Trace Element Determination: A Review. *Appl. Spectrosc. Rev. , 46*, 38-66.

Blumenthal, B., Sellers, K., & Koval, M. (2006). Thallium and Thallium Compounds. *Kirk-Othmer Encycl. Chem. Technol. , 23*, 1-16.

Broekaert, J. A. (2005). *Analytical Atomic Spectrometry with Flames and Plasmas* (Second, Completely Revised and Extended Edition ed.). Weinheim: WILEY-VCH.

Campbell, A. D. (1992). A Critical Survey of Hydride Generation Techniques in Atomic Spectroscopy. *Pure Appl. Chem. , 64*, 227-244.

Dadfarnia, S., Assadollahi, T., & Haji Shabani, A. M. (2007). Speciation and Determination of Thallium by On-line Microcolumn Separation/Preconcentration by Flow Injection-Flame Atomic Absorption Spectrometry Using Immobilized Oxine as Sorbent. *J. Hazard. Mater. , 148*, 446-452.

Das, A. K., Chakraborty, R., Cervera, M. L., & Guardia, M. d. (2006). Determination of Thallium in Biological Samples. *Anal. Bioanal. Chem. , 385*, 665-670.

Dědina, J. (2010). Generation of Volatile Compounds for Analytical Atomic Spectroscopy. *Encyclopedia of Analytical Chemistry* , DOI:10.1002/9780470027318.a9127.

Dědina, J., & Tsalev, D. L. (1995). *Hydride Generation Atomic Absorption Spectrometry.* Chichester: John Wiley & Sons Ltd.

Ebdon, L., Goodal, P., Hill, S. J., Stockwell, P., & Thompson, K. C. (1995). Improved Thallium Hydride Generation Using Continuous Flow Methodologies. *J. Anal. At. Spectrom. , 10*, 317-320.

Ensafı, A. A., & Rezaei, B. (1998). Speciation of Thallium by Flow Injection Analysis with Spectrofluorimetric Detection. *Microchem. J. , 60*, 75-83.

Florence, T. M. (1986). Electrochemical Approaches to Trace Element Speciation in Waters. A Review. *Analyst , 111*, 489-505.

Frech, W., & Baxter, D. C. (1996). Spatial Distributions of Non-atomic Species in Graphite Furnaces. *Spectrochim. Acta, Part B , 51*, 961-972.

Hosseini, M. S., Chamsaz, M., Raissi, H., & Naseri, Y. (2005). Flotation Separation and Electrothermal Atomic Absorption Spectrometric Determination of Thallium in Wastewater Samples. *Anal. Chim. , 96*, 109-116.

Kazantzis, G. (2000). Thallium in the Environment and Health Effects. *Environ. Geochem. Health , 22*, 275-280.

Keith, L. H., & Telliard, W. (1979). ES&T Special Report: Priority Pollutants: I-a Perspective View. *Environ. Sci. Technol. , 13*, 416-423.

Kumar, A. R., & Riyazuddin, P. (2010). Chemical Interferences in Hydride-Generation Atomic Spectrometry. *Trends Anal. Chem. , 29*, 166-176.

Laborda, F., Bolea, E., Baranguan, M. T., & Castillo, J. R. (2002). Hydride Generation in Analytical Chemistry and Nascent Hydrogen: When is it Going to be Over? *Spectrochim. Acta, Part B , 57*, 797-802.

Liao, Y.-P., Chen, G., Yan, D., Li, A.-M., & Ni, Z.-M. (1998). Investigation of Thallium Hydride Generation Using in Situ Trapping in Graphite Tube by Atomic Absorption Spectrometry. *Anal. Chim. Acta , 360*, 209-214.

Lin, T. S., & Nriagu, J. O. (1999). Thallium Speciation in River Waters with Chelex-100 Resin. *Anal. Chim. Acta , 395*, 301-307.

L'vov, B. L. (2005). Fifty Years of Atomic Absorption Spectrometry. *J. Anal. Chem. , 60*, 382-392.

Meeravali, N. N., & Jiang, S.-J. (2008). Ultra-trace Speciation Analysis of Thallium in Environmental Water Samples by Inductively Coupled Plasma Mass Spectrometry After a Novel Sequental Mixed-micelle Cloud Point Extraction. *J. Anal. At. Spectrom. , 23*, 555-560.

Musil, S., Kratzer, J., Vobecký, M., Benada, O., & Matoušek, T. (2010). Silver Chemical Vapor Generation for Atomic Absorption Spectrometry: Minimization of Transport Losses, Interferences and Application to Water Analysis. *J. Anal. At. Spectrom. , DOI: 10.1039/c0ja00018c*.

Pavlíčkova, J., Zbíral, J., Smatanová, M., Habarta, P., Houserová, P., & Kubáň, V. (2006). Uptake of Thallium from Naturally-Contaminated Soils into Vegetables. *Food Addit. Contam. , 23*, 484-491.

Pérez-Ruiz, T., Martínez-Lozano, C., Tomás, V., & Casajús, R. (1996). Simple Flow Injection Spectrofluorimetric Method for Speciation of Thallium. *The Analyst , 121*, 813-816.

Pohl, P. (2004). Recent Advances in Chemical Vapour Generation via Reaction with Sodium tetrahydroborate. *Trends Anal. Chem. , 23*, 21-27.

Scheckel, K. G., Lombi, E., Rock, S. A., & Mclaughlin, M. J. (2004). In Vivo Synchrotron Study of Thallium Speciation and Compartmentation in Iberis Intermedia. *Environ. Sci. Technol. , 38*, 5095-5100.

Shan, X.-Q., Ni, Z.-M., & Zhang, L. (1984). Application of Matrix Modification in Determination of Thallium in Waste Water by Graphite-Furnace Atomic-Absorption Spectrometry. *Talanta , 31*, 150-152.

Slavin, W., & Manning, D. C. (1980). The L'vov Platform for Furnace Atomic Absorption Analysis. *Spectrochim. Acta, Part B , 35*, 701-714.

Sturgeon, R. E., Guo, X., & Mester, Z. (2005). Chemical Vapor Generation: Are Further Advances Yet Possible? *Anal. Bioanal. Chem. , 382*, 881-883.

Tsalev, D. L. (1999). Hyphenated Vapour Generation Atomic Absorption Spectrometric Techniques. *J. Anal. At. Spectrom. , 14*, 147-162.

Vale, M. G., Silva, M. M., Welz, B., & Newka, R. (2002). Control of Spectral and Non-spectral Interferences in the Determination of Thallium in River and Marine Sediments Using Solid Sampling Electrothermal Atomic Absorption Spectrometry. *J. Anal. At. Spectrom. , 17*, 38-45.

Welz, B., & Sperling, M. (1999). *Atomic Absorption Spectrometry* (3 ed.). Weinheim: WILEY-VCH.

Xu, S., Zhou, H., Du, X., & Zhu, D. (2001). Enhancement Reagents for Response Signals of Copper, Gold and Thallium in Flow Injection Vapor Generation AAS. *Chem. J. Int. , 3*, 29-34.

Yan, D., Yan, Z., Cheng, G.-S., & Li, A.-M. (1984). Determination of Indium and Thallium by Hydride Generation and Atomic-Absorption Spectrometry. *Talanta , 31*, 133-134.

Zen, J.-M., & Wu, J.-W. (1997). Square-wave Voltammetric Stripping Analysis of Thallium(III) at a Poly(4-vinylpyridine)/mercury Film Electrode. *Electroanalysis , 9*, 302-306.

Zendelovska, D., & Stafilov, T. (2001). Extraction Separation and Electrothermal Atomic Absorption Spectrometric Determination of Thallium in Some Sulfide Minerals. *Anal. Sci. , 17*, 425-428.

Zhu, D., & Xu, S. (2000). Enhancement of Thallium Response by Flow Injection Hydride Generation AAS Using Palladium and Rhodamine B. *At. Spectrosc. , 21*, 136-142.